5 TWO-SINUSOID-INPUT DESCRIBING FUNCTION (TSIDF)

5.0 INTRODUCTION

Circumstances which lead to periodic but highly nonsinusoidal nonlinearity inputs render the DF approach invalid. In a number of such cases the nonlinearity input is well described as being composed of *two* additive sinusoids. These sinusoids result, in most cases of interest, from a sinusoidal input to the system, from system limit cycles, or both. The input to the nonlinearity is assumed, for the purpose of describing function calculation, to have the form

$$x(t) = A \sin(\omega_A t + \theta_A) + B \sin(\omega_B t + \theta_B) \tag{5.0-1}$$

in which the amplitudes A and B and frequencies ω_A and ω_B will be determined by the nature of the system and its inputs. From the point of view of the general describing function theory developed in Chap. 1, the random variables which characterize this input are the phase angles θ_A and θ_B.

When two or more sinusoidal components are assumed at the nonlinearity input, the statistical independence of these components, which if true

simplifies describing function calculation considerably, must be established with some care. Since each sinusoidal component is characterized by an amplitude and frequency which are deterministically fixed, and by a phase angle, the independence of the input components is established if the phase angles can properly be described as independent random variables. There are a number of important situations in which these phase angles are *not* independent. If one sinusoid were harmonically related to the other, the periods of the sinusoids would be commensurate, and a consistent phase relation would exist between them. The nature of the nonlinearity output would depend on this relative phase, and the quasi-linear approximator should reflect that dependence. In that case, with two sinusoidal inputs, only one phase angle could be treated as a random variable with a uniform distribution over one cycle; the other phase angle would be deterministically related to the first. With the statistical approach of Chap. 1, the coupled set of integral equations indicated in Eq. (1.5-13) would have to be solved to determine the optimum quasi-linear approximator for the nonlinearity. Alternatively, the interpretation of these describing functions as the amplitude and phase relation between each input component and the harmonic component of the same frequency in the nonlinearity output can be employed for describing function calculation. This latter point of view is expressed in the statements

$$N_A = \frac{\text{phasor representation of output component of frequency } \omega_A}{\text{phasor representation of input component of frequency } \omega_A} \tag{5.0-2}$$

$$N_B = \frac{\text{phasor representation of output component of frequency } \omega_B}{\text{phasor representation of input component of frequency } \omega_B} \tag{5.0-3}$$

where the subscript on N denotes the input component to which the describing function applies. These TSIDFs for the case of harmonically related inputs are in general functions of the amplitudes of both input components, the relative phase angle of these sinusoids, and the frequencies of each for a dynamic nonlinearity, the frequency ratio in the case of a static nonlinearity.

When one is studying the effect of a sub- or superharmonic of a sinusoidal signal, the frequencies of the two sinusoids under consideration are locked together into a harmonic relationship. In other cases, the frequencies of the two sinusoids are not locked into such a relation, but are determined, rather, by the nature of the system or its inputs. An example of this would be a limit cycling system responding to a sinusoidal input. One sinusoidal component at the nonlinearity input would have the frequency of the input to the system; the other would have the frequency of the system limit cycle. When the frequencies are determined by two unrelated mechanisms such as these, the periods of the two sinusoids may be thought of as incommensurate,

or the frequency ratio irrational, since the set of rational numbers is a set of zero measure. This means that if the frequencies are determined by unrelated causes, the event that they should be found to be rationally related is an event of zero probability. For sinusoids with incommensurate periods, the concept of a relative phase angle has no meaning, and one may properly think of the phase angles as given independently at random.

Situations in which the frequencies of the sinusoidal components at the nonlinearity input are not related harmonically thus satisfy the assumption of independence which led to the uncoupled expression for the optimum quasi-linear approximator [Eq. (1.5-21)] and its specialization to a sinusoidal input component in the presence of any other uncorrelated inputs [Eq. (1.5-36)], which is repeated here for convenience.

$$N_A = n_p + jn_q \tag{5.0-4a}$$

$$n_p = \frac{2}{A}\overline{y(0)\sin\theta_A} \tag{5.0-4b}$$

$$n_q = \frac{2}{A}\overline{y(0)\cos\theta_A} \tag{5.0-4c}$$

This is the describing function for the transfer of the sinusoidal component with amplitude A. The corresponding describing function for the transfer of the component with amplitude B is given by the same expression, with B replacing A. The indicated expectations in this case represent integrations over the distributions of the two random phase angles, θ_A and θ_B. Thus, for example, if the nonlinearity were static and single-valued, so $y(0)$ were given unambiguously in terms of $x(0)$, n_q would be zero, as was shown in Sec. 1.5, and the describing functions for the two input components would be written

$$N_A = \frac{1}{2\pi^2 A}\int_0^{2\pi} d\theta_A \int_0^{2\pi} d\theta_B\, y(A\sin\theta_A + B\sin\theta_B)\sin\theta_A \tag{5.0-5}$$

$$N_B = \frac{1}{2\pi^2 B}\int_0^{2\pi} d\theta_A \int_0^{2\pi} d\theta_B\, y(A\sin\theta_A + B\sin\theta_B)\sin\theta_B \tag{5.0-6}$$

The probability density functions for θ_A and θ_B have both been written as $1/2\pi$ over the interval $(0,2\pi)$. The integrations could equally well be taken over any other interval which spans one cycle, such as $(-\pi,\pi)$. These TSIDFs can be seen to depend only on the amplitudes of the input components.

An important special case is that in which one of the sinusoids at the

input to the nonlinearity has an infinitesimal amplitude. The quasi-linear gain of the nonlinearity to such an infinitesimal sinusoid in the presence of another is called the *incremental-input describing function.* It is possible to express this describing function in terms of the DF for the nonlinearity.

In this chapter applications of the TSIDF and incremental-input describing function are made to various situations in which DF theory is inadequate. These include the two-sinusoid response of nonlinear systems, subharmonic oscillations, frequency response counterexamples, and multiple limit cycles; other applications are indicated. Jump resonance phenomena and transient oscillations are also briefly treated, despite the fact that we have already developed adequate means for their study via the DF. In the case of jump resonance phenomena a different and possibly more appealing point of view than that presented in Sec. 3.3 is shown to lead to precisely the same result obtained earlier. The study of transient oscillations is directed toward the determination of relative stability of steady-state oscillations. The procedure developed is simple to execute, and is comparable in accuracy with the quasi-static solution of Chap. 4. We begin with a treatment of TSIDF calculation.

5.1 TSIDF CALCULATION

Many different methods for TSIDF calculation are available. In general, they are all more difficult to execute than the various schemes for DF calculation treated in Chap. 2. Certainly, this is to be expected; the problem now under consideration is far more general. Nevertheless, once derived, application of the TSIDF proceeds in a remarkably simple way.

TSIDF CALCULATION BY DIRECT EXPANSION

This method of TSIDF calculation is applicable when representation of the nonlinearity is in terms of a low-order polynomial. The approach is therefore somewhat limited in scope. Nevertheless, this approach leads directly to several interesting results, some of which will be encountered in subsequent sections. Motivated by the work of West, Douce, and Livesley (Ref. 22), we proceed by example.

Example 5.1-1 Consider the cubic characteristic

$$y = x^3 \tag{5.1-1}$$

For an input of the form

$$x = A\cos\omega t + B\cos(\gamma\omega t + \theta) \tag{5.1-2}$$

one may determine output harmonic content by direct expansion, as follows:

$$\begin{aligned} y &= [A\cos\omega t + B\cos(\gamma\omega t + \theta)]^3 \\ &= A^3\cos^3\omega t + 3A^2B\cos^2\omega t\cos(\gamma\omega t + \theta) \\ &\quad + 3AB^2\cos\omega t\cos^2(\gamma\omega t + \theta) + B^3\cos^3(\gamma\omega t + \theta) \\ &= \left(\frac{3A^3}{4} + \frac{3AB^2}{2}\right)\cos\omega t + \frac{A^3}{4}\cos 3\omega t \\ &\quad + \left(\frac{3A^2B}{2} + \frac{3B^3}{4}\right)\cos(\gamma\omega t + \theta) \\ &\quad + \frac{3A^2B}{4}\{\cos[(\gamma + 2)\omega t + \theta] + \cos[(\gamma - 2)\omega t + \theta]\} \\ &\quad + \frac{3AB^2}{4}\{\cos[(2\gamma + 1)\omega t + 2\theta] + \cos[(2\gamma - 1)\omega t + 2\theta]\} \\ &\quad + \frac{B^3}{4}\cos(3\gamma\omega t + 3\theta) \end{aligned} \tag{5.1-3}$$

The last fully expanded equation is written in terms of only single-frequency components. Several distinct cases corresponding to different values of γ are of interest.

Case 1. Non-harmonically-related input sinusoids[1] In this event the only output terms of the same frequency as the input sinusoids are the first and third terms of Eq. (5.1-3). Terming $N_A(A,B)$ and $N_B(A,B)$ the TSIDFs for input frequencies ω and $\gamma\omega$, respectively, gives

$$\begin{aligned} N_A(A,B) &= \frac{3A^3/4 + 3AB^2/2}{A} \\ &= \tfrac{3}{4}A^2 + \tfrac{3}{2}B^2 \end{aligned} \tag{5.1-4}$$

and

$$\begin{aligned} N_B(A,B) &= \frac{3A^2B/2 + 3B^3/4}{B} \\ &= \tfrac{3}{4}B^2 + \tfrac{3}{2}A^2 \end{aligned} \tag{5.1-5}$$

The symmetry between these expressions, both of which are *real*, *independent of* γ, and *independent of* θ, is apparent.

Case 2. Harmonically related input sinusoids ($\gamma = \frac{1}{3}$) The output terms of interest in Eq. (5.1-3) are repeated for convenience:

$$\begin{aligned} y = &\left(\frac{3A^3}{4} + \frac{3AB^2}{2}\right)\cos\omega t + \left(\frac{3A^2B}{2} + \frac{3B^3}{4}\right)\cos(\tfrac{1}{3}\omega t + \theta) \\ &+ \frac{3AB^2}{4}\cos(-\tfrac{1}{3}\omega t + 2\theta) + \frac{B^3}{4}\cos(\omega t + 3\theta) + \text{terms at other frequencies} \end{aligned} \tag{5.1-6}$$

[1] Cases where γ is irrational (e.g., not expressible as the ratio of two integers). Results obtained for the cubic nonlinearity also hold for harmonic frequency ratios (e.g., rational γ), provided $\gamma \neq \frac{1}{3}, 1, 3$.

As varied phase angles are associated with the terms to be considered, the phasor representation called for by Eqs. (5.0-2) and (5.0-3) is conveniently utilized, with the result that

$$N_A(A,B,\tfrac{1}{3},\theta) = \frac{(\frac{3}{4}A^3 + \frac{3}{2}AB^2)e^{j\omega t} + (\frac{1}{4}B^3)e^{j(\omega t+3\theta)}}{Ae^{j\omega t}}$$

$$= \tfrac{3}{4}A^2 + \tfrac{3}{2}B^2 + \tfrac{1}{4}(B^3/A)\, e^{j3\theta} \qquad (5.1\text{-}7a)$$

and

$$N_B(A,B,\tfrac{1}{3},\theta) = \frac{(\frac{3}{2}A^2B + \frac{3}{4}B^3)e^{j[(\omega/3)t+\theta]} + \frac{3}{4}AB^2e^{j[(\omega/3)t-2\theta]}}{Be^{j[(\omega/3)t+\theta]}}$$

$$= \tfrac{3}{2}A^2 + \tfrac{3}{4}B^2 + \tfrac{3}{4}ABe^{-j3\theta} \qquad (5.1\text{-}7b)$$

The TSIDFs are both *complex* and *dependent* upon θ.

Case 3. Harmonically related input sinusoids ($\gamma = 3$) This case is, essentially, identical with Case 2, with the roles of the higher- and the lower-frequency input terms reversed. It warrants no further discussion.

TSIDF CALCULATION BY DOUBLE FOURIER SERIES EXPANSION

This calculation is based on a procedure described by Bennett (Ref. 2), and later by Kalb and Bennett (Ref. 14). Corresponding to the input

$$x(t) = A \sin \omega t + B \sin (\gamma\omega t + \theta) \qquad (5.1\text{-}8)$$

the nonlinearity output is sought in the form

$$y(t) = y(A \sin \psi_1 + B \sin \psi_2)$$

$$= \sum_{m=0}^{\infty} \sum_{\substack{n=-\infty\,(m\neq 0)\\ n=0\,(m=0)}}^{\infty} [P_{mn} \sin (m\psi_1 + n\psi_2) + Q_{mn} \cos (m\psi_1 + n\psi_2)] \qquad (5.1\text{-}9)$$

where $\psi_1 = \omega t$ and $\psi_2 = \gamma\omega t + \theta$

The Fourier coefficients P_{mn} and Q_{mn} are determined in the usual manner by multiplying both sides of Eq. (5.1-9) by the multiplier of the coefficient which is to be found, and integrating the result throughout the square bounded by $\psi_1 = \pm\pi$, $\psi_2 = \pm\pi$. This yields

$$P_{mn} = \frac{1}{2\pi^2} \int_{-\pi}^{\pi}\int y(A \sin \psi_1 + B \sin \psi_2) \sin (m\psi_1 + n\psi_2)\, d\psi_1\, d\psi_2 \qquad (5.1\text{-}10)$$

and

$$Q_{mn} = \frac{1}{2\pi^2} \int_{-\pi}^{\pi}\int y(A \sin \psi_1 + B \sin \psi_2) \cos (m\psi_1 + n\psi_2)\, d\psi_1\, d\psi_2 \qquad (5.1\text{-}11)$$

In the case of static single-valued nonlinearities, an important property of Q_{mn} can be demonstrated by rewriting Eq. (5.1-11) as four integrals covering the ranges $-\pi/2 < \psi_1 < 3\pi/2$ and $-\pi/2 < \psi_2 < 3\pi/2$.

$$\begin{aligned} 2\pi^2 Q_{mn} &= \int_{-\pi/2}^{\pi/2} d\psi_2 \int_{-\pi/2}^{\pi/2} d\psi_1 [y(A \sin \psi_1 + B \sin \psi_2) \cos (m\psi_1 + n\psi_2)] \\ &\quad + \int_{-\pi/2}^{\pi/2} d\psi_2 \int_{\pi/2}^{3\pi/2} d\psi_1 [\ ] \\ &\quad + \int_{\pi/2}^{3\pi/2} d\psi_2 \int_{-\pi/2}^{\pi/2} d\psi_1 [\ ] + \int_{\pi/2}^{3\pi/2} d\psi_2 \int_{\pi/2}^{3\pi/2} d\psi_1 [\ ] \\ &= I_1 + I_2 + I_3 + I_4 \end{aligned} \tag{5.1-12}$$

The integrand, unchanged from one integral to the next, has been denoted by brackets. In I_3 and I_4, the last two terms in Eq. (5.1-12), we make the substitutions

$$\psi_1^* = \pi - \psi_1 \qquad \text{and} \qquad \psi_2^* = \pi - \psi_2$$

which result in the determination that

$$I_3 + I_4 = \cos (m + n)\pi \, (I_1 + I_2)$$

Hence Q_{mn} can be written as

$$Q_{mn} = \frac{1 + \cos (m + n)\pi}{2\pi^2} (I_1 + I_2)$$

whence it follows that

$$Q_{mn} = 0 \qquad \text{for } m + n \text{ odd} \tag{5.1-13}$$

Beginning with Eq. (5.1-10) and pursuing a similarly constructed argument, it is also readily demonstrated that

$$P_{mn} = 0 \qquad \text{for } m + n \text{ even}$$

If, in addition, the nonlinearity is odd, it can be further proved that *all* $Q_{mn} = 0$.

Let us return to Eq. (5.1-9) and note that, for γ irrational, the only output term of frequency ω occurs for $m = 1$, $n = 0$. Correspondingly, the only output term of frequency $\gamma\omega$ occurs for $m = 0$, $n = 1$. In each of these instances it follows from previous arguments that $Q_{mn} = 0$. Hence we arrive at the TSIDF expressions

$$\begin{aligned} N_A(A,B) &= \frac{P_{10}}{A} \\ &= \frac{1}{2\pi^2 A} \int_{-\pi}^{\pi} \int_{-\pi}^{\pi} y(A \sin \psi_1 + B \sin \psi_2) \sin \psi_1 \, d\psi_1 \, d\psi_2 \end{aligned} \tag{5.1-14}$$

and $$N_B(A,B) = \frac{P_{01}}{B}$$

$$= \frac{1}{2\pi^2 B} \int_{-\pi}^{\pi}\int y(A \sin \psi_1 + B \sin \psi_2) \sin \psi_2 \, d\psi_1 \, d\psi_2 \quad (5.1\text{-}15)$$

These TSIDFs are real numbers. They are independent of θ and γ, and dependent only upon A and B. These expressions are exactly those of Eqs. (5.0-5) and (5.0-6), which result from the unified theory of Chap. 1.

If γ is rational, more than one term of Eq. (5.1-9) yields the frequency of interest. Calculating $N_A(A,B)$, for example, we look for all terms for which

$$m\omega + n\gamma\omega = \omega$$

or

$$n = \frac{1}{\gamma}(1 - m) \quad (5.1\text{-}16)$$

Thus, when $\gamma = \frac{1}{3}$, the pairs of values (m,n) which satisfy Eq. (5.1-16) are (0,3), (1,0), (2, −3), (3, −6), etc.; and for $\gamma = 3$, the appropriate pairs are (1,0), (4, −1), (7, −2), (10, −3), etc. In each of these terms $Q_{mn} = 0$, and the component of $y(t)$ at frequency ω is computed from Eq. (5.1-9) as

$$\begin{aligned} y(t) &= \sum_m P_{mn} \sin \left\{ m\omega t + \left[\frac{1}{\gamma}(1 - m)\right]\gamma\omega t + \left[\frac{1}{\gamma}(1 - m)\right]\theta \right\} \\ &= \sum_m P_{mn} \sin \left[\omega t + \frac{1}{\gamma}(1 - m)\theta \right] \\ &= P_N \sin (\omega t + \theta_N) \end{aligned}$$

The TSIDF is therefore given by

$$N_A(A,B) = \frac{P_N(A,B,\gamma,\theta)}{A} e^{j\theta_N(A,B,\gamma,\theta)}$$

which is complex and dependent upon γ and θ, in addition to A and B.

Example 5.1-2 Consider the ideal-relay characteristic defined by

$$y(A \sin \psi_1 \pm B \sin \psi_2) = \begin{cases} D & \text{for } \sin \psi_1 \pm k \sin \psi_2 \geq 0 \\ -D & \text{for } \sin \psi_1 \pm k \sin \psi_2 < 0 \end{cases}$$

where $k = B/A$, and for the present development we adopt the convention that A corresponds to the larger sinusoid. This ensures a solution to the switching condition $\sin \psi_1 \pm k \sin \psi_2 = 0$. In order to calculate $N_A(A,B)$, the double-integral formulation of Eq. (5.1-14) is written as follows:

$$N_A(A,B) = \frac{1}{2\pi^2 A}\left(\int_{-\pi}^{0} d\psi_2 \int_{-\pi}^{0} d\psi_1 [\ ] + \int_{-\pi}^{0} d\psi_2 \int_{0}^{\pi} d\psi_1 [\ ] \right.$$

$$\left. + \int_{0}^{\pi} d\psi_2 \int_{-\pi}^{0} d\psi_1 [\ ] + \int_{0}^{\pi} d\psi_2 \int_{0}^{\pi} d\psi_1 [\ ] \right)$$

where, as before, the integrand is denoted simply by brackets. Changes of variable are now effected in the first three integrals, to convert all the limits of integration to the range 0 to π. Using the property of odd characteristics, $y(x) = -y(-x)$, the result of this manipulation is expressible as

$$N_A(A,B) = \frac{1}{\pi^2 A}\int_0^{\pi} d\psi_2 \int_0^{\pi} d\psi_1 \sin\psi_1 [y(A\sin\psi_1 + B\sin\psi_2) + y(A\sin\psi_1 - B\sin\psi_2)]$$

The calculation attendant on this integral formulation can be somewhat simplified by recasting it into four double integrals, each of $\pi/2$-radian range in the independent variables ψ_1 and ψ_2. Operating on these integrals by appropriate variable substitutions so as to achieve a range of integration 0 to $\pi/2$ in ψ_1 and ψ_2, and collecting the results, yields

$$N_A(A,B) = \frac{4}{\pi^2 A}\int_0^{\pi/2} d\psi_2 \int_0^{\pi/2} d\psi_1 \sin\psi_1 [y(A\sin\psi_1 + B\sin\psi_2) + y(A\sin\psi_1 - B\sin\psi_2)]$$

As this formulation has not yet been specialized other than to odd memoryless characteristics, observe that it is generally applicable. We now proceed to the specific ideal-relay nonlinearity.

Over the entire range 0 to $\pi/2$ in each of the angles ψ_1 and ψ_2, $y(A\sin\psi_1 + B\sin\psi_2) = D$. However, $y(A\sin\psi_1 - B\sin\psi_2)$ assumes both of the values $\pm D$, depending upon the sign of its argument. The angle which satisfies the switching condition $\sin\psi_1 - k\sin\psi_2 = 0$ is $\psi_1 = \sin^{-1}(k\sin\psi_2)$. Therefore we can write

$$\begin{aligned} N_A(A,B) &= \frac{4D}{\pi^2 A}\int_0^{\pi/2} d\psi_2 \left(\int_0^{\pi/2} \sin\psi_1\, d\psi_1 \right. \\ &\qquad \left. - \int_0^{\sin^{-1}(k\sin\psi_2)} \sin\psi_1\, d\psi_1 + \int_{\sin^{-1}(k\sin\psi_2)}^{\pi/2} \sin\psi_1\, d\psi_1 \right) \\ &= \frac{8D}{\pi^2 A}\int_0^{\pi/2} \cos[\sin^{-1}(k\sin\psi_2)]\, d\psi_2 \\ &= \frac{8D}{\pi^2 A}\int_0^{\pi/2} \sqrt{1 - k^2\sin^2\psi_2}\, d\psi_2 \\ &= \frac{8D}{\pi^2 A} E(k) \end{aligned} \tag{5.1-17a}$$

where $E(k)$ is the complete elliptic integral of the first kind. Denoting by $K(k)$ the complete elliptic integral of the second kind, it is readily proved that

$$N_B(A,B) = \frac{8D}{\pi^2 k^2 A}[E(k) - (1-k^2)K(k)] \tag{5.1-17b}$$

where
$$E(k) = \int_0^{\pi/2} \sqrt{1 - k^2\sin^2\psi}\, d\psi \qquad K(k) = \int_0^{\pi/2} \frac{d\psi}{\sqrt{1 - k^2\sin^2\psi}} \tag{5.1-18}$$

It is to be observed that N_A and N_B are indeed both real and independent of frequency. Expansion of these functions in powers of k yields

$$N_A(A,B) = \frac{4D}{\pi A}\left(1 - \frac{1}{4}k^2 - \frac{3}{64}k^4 - \frac{5}{256}k^6 - \cdots\right) \tag{5.1-19a}$$

$$N_B(A,B) = \frac{2D}{\pi A}\left(1 + \frac{1}{8}k^2 + \frac{3}{64}k^4 + \frac{25}{1{,}024}k^6 + \cdots\right) \tag{5.1-19b}$$

whence we deduce the useful relationship

$$\frac{N_B(A,B)}{N_A(A,B)} \approx \frac{1}{2} \qquad \text{for } k < 1 \tag{5.1-20}$$

Calculation of the TSIDFs for harmonically related input sinusoids can be pursued as outlined earlier in the text or by single Fourier series expansion techniques. Rather than present details of the calculation here, we simply observe that the TSIDFs are now complex and dependent upon A, B, γ, and θ. It is of interest to note the *maximum* phase shift associated with $N_B(A,B,\gamma,\theta)$. The absolute value of this phase shift appears in Table 5.1-1 for various values of γ. It can be seen that, for a given k, the largest values occur at $\gamma = \frac{1}{3}$. For $k \leq 0.5$ and $\gamma \leq \frac{1}{5}$, this phase shift is less than 0.5°.

TABLE 5.1-1 MAXIMUM PHASE SHIFT IN $N_B(A,B,\gamma,\theta)$ FOR AN IDEAL RELAY†

γ	Maximum phase shift
$\frac{1}{3}$	$\tan^{-1}\frac{k}{4}$
$\frac{1}{2}$	$\tan^{-1}\frac{k}{8}$
$\frac{1}{5}$	$\tan^{-1}\frac{k}{64}$

† Amsler and Gorozdos, Ref. 1.

In the single-sinusoid-input case the nonlinearity output harmonics and the filtering properties of the loop linear elements determine whether DF analysis is valid. The familiar desired filtering property of the linear elements is amplitude attenuation with increasing frequency. In the two-sinusoid-input case a slightly different situation arises. This is a consequence of the fact that nonlinearity output terms can occur at frequencies *below* and *between*, as well as *above*, the input frequencies. In other words, because of the modulation process taking place, both sum and difference frequency terms are created. The sum frequency terms are necessarily at higher frequencies than either input sinusoid; hence for these terms the usual low-pass-filter requirement is necessary to validate TSIDF analysis. The difference frequency terms can be additionally troublesome, however, particularly if the loop linear elements have a resonance peak at one or more of these frequencies. It is certainly obvious at this point that to determine all these terms would be a monumental chore. In theory, all that is required is the evaluation of each term P_{mn} (and Q_{mn}) of interest. In practice, this determination is usually intractable.

Often the difference frequency terms are of quite small amplitude. This is particularly true when the frequency ratio γ is either very large or very

TABLE 5.1-2 OUTPUT OF AN IDEAL RELAY IN RESPONSE TO A TEST INPUT

Individual sinusoidal output components

Frequency	Amplitude
1	0.128
2	0.000
3	0.000
4	0.000
5	0.000
6	0.000
7	0.000
8	0.006
9	0.000
10	1.260
11	0.000
12	0.006

small. In support of this statement there is listed in Table 5.1-2 the output of an ideal relay (drive levels ± 1) in response to an input

$$x = 0.2 \sin t + \sin 10t$$

For all practical purposes there is *no* output harmonic distortion. At the frequencies $\omega = 1$ and $\omega = 10$, however, significant amplitudes do occur. These are very well predicted by Eqs. (5.1-19), the solutions derived for non-harmonically-related input sinusoids. That they also apply to the case of harmonically related input sinusoids will be explained in subsequent discussions of TSIDF approximation.

TSIDF CALCULATION BY INTEGRAL REPRESENTATION

This method has been employed by Gibson and Sridhar (Ref. 10) for the case of non-harmonically-related input sinusoids, using techniques of random-process theory. Below, we develop the TSIDFs for non-harmonically-related input sinusoids with the aid of completely deterministic arguments.

The output of an instantaneous nonlinear element can be written as a function of the input using the integral representation

$$y(x) = \frac{1}{2\pi} \int_{-\infty}^{\infty} Y(ju) \exp(jux)\, du \tag{5.1-21}$$

where $Y(ju)$ is the Fourier transform of $y(x)$,

$$Y(ju) = \int_{-\infty}^{\infty} y(x) \exp(-jux)\, dx \tag{5.1-22}$$

The convergence of this integral can usually be enforced artificially, as is subsequently demonstrated by example. If $y(x)$ is an odd function of x (odd nonlinear characteristic), $Y(ju)$ is an odd function of u. In the following discussion only odd characteristics are considered. The nonlinearity input is taken in the form

$$x = A \sin \omega t + B \sin \gamma \omega t \tag{5.1-23}$$

where γ is *not* rational. From Eq. (5.1-21) the corresponding output is

$$\begin{aligned} y &= \frac{1}{2\pi} \int_{-\infty}^{\infty} Y(ju) \exp (jAu \sin \omega t + jBu \sin \gamma \omega t)\, du \\ &= \frac{1}{2\pi} \int_{-\infty}^{\infty} Y(ju) \exp (jAu \sin \omega t) \exp (jBu \sin \gamma \omega t)\, du \end{aligned} \tag{5.1-24}$$

A key point in this development, due to Rice (Ref. 20), is the use of an expansion of the exponentials in series of the form (Ref. 5)

$$\begin{aligned} \exp (j\alpha \sin \beta) &= \cos (\alpha \sin \beta) + j \sin (\alpha \sin \beta) \\ &= \sum_{n=0}^{\infty} \epsilon_n J_{2n}(\alpha) \cos 2n\beta + 2j \sum_{n=0}^{\infty} J_{2n+1}(\alpha) \sin (2n+1)\beta \end{aligned} \tag{5.1-25}$$

where ϵ_n denotes the Neumann factor

$$\epsilon_n = \begin{cases} 1 & \text{for } n = 0 \\ 2 & \text{for } n = 1, 2, 3, \ldots \end{cases}$$

and $J_\nu(\alpha)$ is the Bessel function of order ν and argument α. Substituting for the exponential terms in Eq. (5.1-24) gives

$$\begin{aligned} &\exp (jAu \sin \omega t) \exp (jBu \sin \gamma \omega t) \\ &= \left[\sum_{m=0}^{\infty} \epsilon_m J_{2m}(Au) \cos 2m\omega t + 2j \sum_{m=0}^{\infty} J_{2m+1}(Au) \sin (2m+1)\omega t \right] \\ &\quad \times \left[\sum_{n=0}^{\infty} \epsilon_n J_{2n}(Bu) \cos 2n\gamma \omega t + 2j \sum_{n=0}^{\infty} J_{2n+1}(Bu) \sin (2n+1)\gamma \omega t \right] \end{aligned} \tag{5.1-26}$$

Since $Y(ju)$ is an odd function of u, only the odd terms in Eq. (5.1-26) contribute to the value of the integral in Eq. (5.1-24). All even functions of u in Eq. (5.1-26), when multiplied by $Y(ju)$, result in integrands in Eq. (5.1-24) which are odd functions of u; the value of the integral over the *doubly* infinite range is then zero. Using the fact that Bessel functions of odd

order are odd, and those of even order are even, yields that the portion of $\exp(jAu \sin \omega t) \exp(jBu \sin \gamma\omega t)$ displaying an odd dependence upon u is

$$2j \sum_{m=0}^{\infty} \sum_{n=0}^{\infty} \epsilon_m J_{2m}(Au) J_{2n+1}(Bu) \cos 2m\omega t \sin (2n+1)\gamma\omega t$$
$$+ 2j \sum_{m=0}^{\infty} \sum_{n=0}^{\infty} \epsilon_n J_{2n}(Bu) J_{2m-1}(Au) \cos 2n\gamma\omega t \sin (2m+1)\omega t \quad (5.1\text{-}27)$$

Employing the trigonometric identity

$$\cos \alpha \sin \beta = \tfrac{1}{2}[\sin (\alpha + \beta) - \sin (\alpha - \beta)]$$

enables rewriting Eq. (5.1-27) in the form

$$j \sum_{m=0}^{\infty} \sum_{n=0}^{\infty} \epsilon_m J_{2m}(Au) J_{2n+1}(Bu)[\sin (2m + 2n\gamma + \gamma)\omega t - \sin (2m - 2n\gamma - \gamma)\omega t]$$
$$+ j \sum_{m=0}^{\infty} \sum_{n=0}^{\infty} \epsilon_n J_{2n}(Bu) J_{2m+1}(Au)$$
$$\times [\sin (2m + 2n\gamma + 1)\omega t - \sin (2n\gamma - 2m - 1)\omega t] \quad (5.1\text{-}28)$$

Suppose that we seek the first-harmonic gain of the nonlinearity. Then the only terms in Eq. (5.1-28) of interest are those involving $\sin \omega t$ or $\sin (-\omega t)$. Considering γ irrational, such terms arise (over the allowable values of the indices m and n) only for the combination $m = 0$, $n = 0$. Had the nonlinearity gain to the input component of frequency $\gamma\omega$ been sought, again only $m = 0$, $n = 0$ would be pertinent. For these cases, therefore, the only terms of interest in Eq. (5.1-28) are

$$2jJ_0(Bu)J_1(Au) \sin \omega t + 2jJ_0(Au)J_1(Bu) \sin \gamma\omega t \quad (5.1\text{-}29)$$

Finally, from Eqs. (5.1-24) and (5.1-29), the *frequency-independent* TSIDF for the fundamental output term is given by

$$N_A(A,B) = \frac{j}{\pi A} \int_{-\infty}^{\infty} Y(ju) J_0(Bu) J_1(Au)\, du \quad (5.1\text{-}30)$$

Similarly,

$$N_B(A,B) = \frac{j}{\pi B} \int_{-\infty}^{\infty} Y(ju) J_0(Au) J_1(Bu)\, du \quad (5.1\text{-}31)$$

We may conclude that the frequency-independent TSIDF expressions for each input component are *functionally identical.* That is,

$$N_A(A,B) = N_B(B,A) \quad (5.1\text{-}32)$$

The only distinction between the two inputs in this case is their relative amplitudes! This conclusion is equally evident from Eqs. (5.1-14) and (5.1-15).

The foregoing procedure can be extended to the case of harmonically related input sinusoids simply by the inclusion of a phase-shift variable in one of the input components and the consideration of rational values of γ (Ref. 18).

Example 5.1-3 As an example of the application of this method, consider the *ideal-relay characteristic*, defined by

$$y(x) = \begin{cases} -De^{\sigma x} & x < 0 \\ 0 & x = 0 \\ De^{-\sigma x} & x > 0 \end{cases}$$

For $\sigma = 0$ this characterization reduces to that for the ideal relay. However, for σ positive, albeit infinitesimal, $y(x)$ as defined above becomes Fourier-transformable. Thus, from Eq. (5.1-22),

$$\begin{aligned} Y(ju) &= \lim_{\sigma \to 0} \left(\int_{-\infty}^{0-} -De^{\sigma x} e^{-jux}\, dx + \int_{0-}^{0+} 0\, dx + \int_{0+}^{\infty} De^{-\sigma x} e^{-jux}\, dx \right) \\ &= \lim_{\sigma \to 0} \left(\frac{1}{j} \frac{2Du}{\sigma^2 + u^2} \right) \\ &= \frac{2D}{ju} \end{aligned} \tag{5.1-33}$$

Equations (5.1-31) and (5.1-33) are evidence that $N_B(A,B)$ is given by

$$N_B(A,B) = \frac{2D}{\pi B} \int_{-\infty}^{\infty} \frac{J_0(Au) J_1(Bu)}{u}\, du \tag{5.1-34}$$

Evaluation of this integral yields

$$N_B(A,B) = \begin{cases} \dfrac{8D}{\pi^2 B} E\left(\dfrac{A}{B}\right) & \text{for } \dfrac{B}{A} > 1 \quad (5.1\text{-}35) \\ \dfrac{8D}{\pi^2 B} \dfrac{A}{B} \left[E\left(\dfrac{B}{A}\right) - \left(1 - \dfrac{B^2}{A^2}\right) K\left(\dfrac{B}{A}\right) \right] & \text{for } \dfrac{B}{A} < 1 \quad (5.1\text{-}36) \end{cases}$$

where the complete elliptic integrals E and K are as defined previously.

The reader may be interested to compare this result with that obtained via double Fourier series expansion. Using the definition $k = B/A$, both results are seen to be identical.

Generally speaking, the transform approach to TSIDF calculation is quite useful. The transformed functions $Y(ju)$ are readily obtained. The major difficulty with this formulation is in evaluating the inversion integrals of Eqs. (5.1-30) and (5.1-31). Often, this can be accomplished in closed form in terms of known functions (gamma functions, hypergeometric functions, and elliptic integrals).

POWER-SERIES EXPANSION

A particularly simple TSIDF calculation mechanism for odd nonlinearities with non-harmonically-related input sinusoids results from the development of $N_A(A,B)$ and $N_B(A,B)$ [Eqs. (5.1-30) and (5.1-31)] in power series. The major steps in this development are briefly sketched in the ensuing presentation.

Let A denote the larger input sinusoid amplitude, and B denote the smaller. Then, provided that the necessary derivatives exist, $N_A(A,B)$ can be expanded in a Taylor series about $B = 0$.

$$N_A(A,B) = \sum_{n=0}^{\infty} \frac{1}{n!} \frac{\partial^n N_A(A,B)}{\partial B^n}\bigg|_{B=0} B^n \tag{5.1-37}$$

The derivatives are computed in the form

$$\frac{\partial^n N_A(A,B)}{\partial B^n} = \frac{j}{\pi A} \int_{-\infty}^{\infty} Y(ju) \frac{\partial^n J_0(Bu)}{\partial B^n} J_1(Au)\, du \tag{5.1-38}$$

Expressing $J_0(Bu)$ in its power series,

$$J_0(Bu) = \sum_{k=0}^{\infty} \frac{(-1)^k (Bu)^{2k}}{2^{2k}(k!)^2} \tag{5.1-39}$$

one can readily demonstrate that

$$\frac{\partial^n J_0(Bu)}{\partial B^n}\bigg|_{B=0} = \begin{cases} 0 & \text{for } n \text{ odd} \qquad (5.1\text{-}40a) \\ \dfrac{(-1)^{n/2} n!\, u^n}{2^n [(n/2)!]^2} & \text{for } n \text{ even} \qquad (5.1\text{-}40b) \end{cases}$$

Thus Eq. (5.1-37) can be rewritten as

$$N_A(A,B) = \frac{j}{\pi A} \sum_{p=0}^{\infty} \frac{(-1)^p B^{2p}}{2^{2p}(p!)^2} \int_{-\infty}^{\infty} Y(ju) J_1(Au) u^{2p}\, du \tag{5.1-41}$$

The dummy variable n has been replaced by p, where $n = 2p$. The integral in this formulation has a surprisingly simple interpretation. This can be seen by first noting that $N_A(A,0)$, the leading term in the series, is the single-input-sinusoid DF, $N(A)$.

$$\begin{aligned} N(A) &= \lim_{B \to 0} N_A(A,B) \\ &= \frac{j}{\pi A} \int_{-\infty}^{\infty} Y(ju) J_1(Au)\, du \end{aligned} \tag{5.1-42}$$

Use has been made of the fact that $J_0(0) = 1$. Repeated differentiation of this equation with respect to A yields relationships which can be so combined that the integral in Eq. (5.1-41) is expressed in terms of the DF and its derivatives! The result of this process is

$$N_A(A,B) = \sum_{p=0}^{\infty} \frac{B^{2p}}{2^{2p}(p!)^2} V_p(A) \tag{5.1-43a}$$

where $V_p(A)$ is computed *recursively* as

$$V_{p+1}(A) = \frac{d^2V_p(A)}{dA^2} + \frac{3}{A}\frac{dV_p(A)}{dA} \tag{5.1-43b}$$

with

$$V_0(A) = N(A) \tag{5.1-43c}$$

In a completely similar way one can show that

$$N_B(A,B) = \sum_{p=0}^{\infty} \frac{B^{2p}}{2^{2p}p!\,(p+1)!} W_p(A) \tag{5.1-44a}$$

where

$$W_{p+1}(A) = \frac{d^2W_p(A)}{dA^2} + \frac{1}{A}\frac{dW_p(A)}{dA} \tag{5.1-44b}$$

and

$$W_0(A) = N(A) + \frac{A}{2}\frac{dN(A)}{dA} \tag{5.1-44c}$$

Although these results may look cumbersome, they are actually quite simple to employ. Their utility is demonstrated by the following examples.

Example 5.1-4 Compute the TSIDFs for a cubic characteristic, $y = x^3$.

The corresponding DF is $N(A) = \frac{3}{4}A^2$. Thus, from Eqs. (5.1-43*c*) and (5.1-44*c*),

$$V_0 = \tfrac{3}{4}A^2 \qquad \text{and} \qquad W_0 = \tfrac{3}{2}A^2$$

Employing the recursive formulations for V_{p+1} and W_{p+1} [Eqs. (5.1-43*b*) and (5.1-44*b*)] gives

$$V_1 = W_1 = 6$$

$$V_p = W_p = 0 \qquad \text{for all } p \geq 2$$

Substitution of these results into the power-series TSIDF expressions [Eqs. (5.1-43*a*) and (5.1-44*a*)] gives

$$N_A(A,B) = \tfrac{3}{4}A^2 + \tfrac{3}{2}B^2$$

$$N_B(A,B) = \tfrac{3}{2}A^2 + \tfrac{3}{4}B^2$$

These expressions are valid for all A, B and are identical with the cubic characteristic TSIDFs computed previously by direct expansion.

Example 5.1-5 Compute the TSIDFs for an ideal relay with drive levels $\pm D$.

Proceeding as above, but with $N(A) = 4D/\pi A$, yields

$$V_0 = \frac{4D}{\pi A} \qquad W_0 = \frac{2D}{\pi A}$$

$$V_1 = \frac{-4D}{\pi A^3} \qquad W_1 = \frac{2D}{\pi A^3}$$

$$V_2 = \frac{-12D}{\pi A^5} \qquad W_2 = \frac{18D}{\pi A^5}$$

. . . . . .

The TSIDF power-series expressions are therefore

$$N_A(A,B) = \frac{4D}{\pi A}\left[1 - \frac{1}{4}\left(\frac{B}{A}\right)^2 - \frac{3}{64}\left(\frac{B}{A}\right)^4 - \frac{5}{256}\left(\frac{B}{A}\right)^6 - \cdots\right]$$

$$N_B(A,B) = \frac{2D}{\pi A}\left[1 + \frac{1}{8}\left(\frac{B}{A}\right)^2 + \frac{3}{64}\left(\frac{B}{A}\right)^4 + \frac{25}{1{,}024}\left(\frac{B}{A}\right)^6 + \cdots\right]$$

The ratio test for infinite series can be employed to determine that each of the above expansions is convergent for $(B/A)^2 < 1$. These expressions are identical with those determined by double Fourier series expansion [Eqs. (5.1-19*a*) and (5.1-19*b*)].

Example 5.1-6 Compute the TSIDFs for the harmonic nonlinearity, $y = \sin mx$.

The required DF is $N(A) = 2J_1(mA)/A$. Application of the differential relationships

$$\frac{dJ_1(mA)}{dA} = -\frac{J_1(mA)}{A} + mJ_0(mA) \qquad \frac{dJ_0(mA)}{dA} = -J_1(mA)$$

yields

$$V_0 = \frac{2J_1(mA)}{A} \qquad W_0 = mJ_0(mA)$$

$$V_1 = \frac{-2m^2J_1(mA)}{A} \qquad W_1 = -m^3J_0(mA)$$

$$V_2 = \frac{2m^4J_1(mA)}{A} \qquad W_2 = m^5J_0(mA)$$

. . . . . .

$$V_p = (-1)^p 2m^{2p}\frac{J_1(mA)}{A} \qquad W_p = (-1)^p m^{2p+1}J_0(mA)$$

Substituting for V_p in Eq. (5.1-43*a*) gives

$$N_A(A,B) = \frac{2}{A}J_1(mA)\sum_{p=0}^{\infty}\frac{(-1)^p(mB)^{2p}}{2^{2p}(p!)^2} =$$

$$= \frac{2}{A}J_1(mA)J_0(mB)$$

upon identification of the infinite series for $J_0(mB)$. Similarly,

$$N_B(A,B) = \frac{2}{B}J_1(mB)J_0(mA)$$

These expressions exist for all A, B and are indeed the exact TSIDFs for the harmonic characteristic (cf. Prob. 5-3).

OTHER METHODS OF TSIDF CALCULATION

One obvious means of TSIDF calculation is by a digital-computer-implemented Fourier series analysis of the actual nonlinearity output. This approach has been used by Jaffe (Ref. 13), Elgerd (Ref. 8), and others for the study of various nonlinear elements. It has the disadvantage that closed-form solutions are never arrived at. On the other hand, it has the far-reaching advantage that it is applicable to *any* nonlinearity whose output is pointwise-determinable in terms of its input.

There remains one additional TSIDF calculation of interest. We defer this to the next chapter, where it is proved that the TSIDF can be computed as the DF of a DIDF, the last-mentioned describing function being the subject of that chapter.

Normalized TSIDF graphs for five common nonlinearities are presented in Appendix D.

5.2 SUBHARMONIC OSCILLATIONS

Systems with suitable nonlinear characteristics can respond to an input sinusoid by producing an output whose lowest-frequency component is a submultiple of the input frequency. The lowest-frequency component is usually at or near the system natural frequency of oscillation. This frequency response phenomenon is thus known as *subharmonic resonance*. Subharmonic frequencies as low as one-thirteenth of the input frequency have been observed in simple systems. Because of the resonant nature of the phenomenon, the subharmonic component is often of large amplitude, causing the system output to bear little resemblance to a sinusoid of the input frequency. Interestingly enough, just outside the region of subharmonic oscillation, the sinusoidally forced system output may be so small as to be practically zero. Complete treatments of subharmonic response phenomena in the cases of smooth and piecewise-linear nonlinearities can be found elsewhere (Refs. 11, 18). For ease in presentation, the TSIDF treatment here is based upon a cubic nonlinearity.

We have already computed the one-third-subharmonic TSIDF in systems with a cubic nonlinearity [Eq. (5.1-7*b*)]. It is rewritten here:

$$N_B(A,B,\tfrac{1}{3},\theta) = \tfrac{3}{4}(B^2 + 2A^2 + AB\cos 3\theta - jAB\sin 3\theta) \qquad (5.2\text{-}1)$$

Call the phase shift of this TSIDF β. It follows that ($k = B/A$)

$$\tan\beta = \frac{-k\sin 3\theta}{2 + k^2 + k\cos 3\theta} \qquad (5.2\text{-}2)$$

This function, maximized over θ, is

$$\tan \beta_{\max \theta} = \frac{-k}{\sqrt{4 + 3k^2 + k^4}} \tag{5.2-3}$$

which can be further extremized with respect to k. Considering real k, Eq. (5.2-3) yields, for $k^2 = 2$,

$$\begin{aligned} \beta_{\max \theta, k} &= \pm \tan^{-1} \sqrt{\tfrac{1}{7}} \\ &\approx \pm 21^\circ \end{aligned} \tag{5.2-4}$$

Hence the *maximum possible* TSIDF phase shift is 21°. To avoid a one-third-subharmonic oscillation, the loop linear elements must have a phase lag *not exceeding* 159°. Under this condition the total phase shift is less than 180°, and oscillation cannot ensue (see Fig. 5.2-1).

Now consider the frequency locus $L(j\omega)$, for which one-third-subharmonic oscillations are possible at input frequencies between $3\omega_1$ and $3\omega_2$ radians/sec. Corresponding to some input frequency ω within this range, $L(j\omega/3)$ provides in excess of 159° phase lag. $N_B(A,B,\frac{1}{3},\theta)$ need therefore only provide an additional phase lag of *less than* 21° for a one-third-subharmonic oscillation to take place. The governing equations are (for a unity feedback configuration)

$$A = \frac{M_r}{|1 + N_A(A,B,\tfrac{1}{3},\theta)L(j\omega)|} \tag{5.2-5}$$

and

$$L(j\omega/3) = \frac{-1}{N_B(A,B,\tfrac{1}{3},\theta)} \tag{5.2-6}$$

At any given ω, a range of subharmonic-oscillation amplitudes can exist as M_r is varied. Stability of a particular subharmonic oscillation is treated in terms of Eqs. (5.2-5) and (5.2-6) and the usual quasi-static describing function argument. It is to be noted that, as the phase of $N_B(A,B,\frac{1}{3},\theta)$ is small for small values of B, the subharmonic oscillation is not self-starting, and must be initiated by some transient within the system.

Example 5.2-1 Determine all pairs of input amplitude and frequency such that the system of Fig. 5.2-2 can exhibit subharmonic oscillations.

We note that Eq. (5.2-6) implies the angle and magnitude conditions

$$\angle L(j\omega/3) + \angle N_B(A,B,\tfrac{1}{3},\theta) = -\pi \tag{5.2-7a}$$

and

$$|L(j\omega/3)|\,|N_B(A,B,\tfrac{1}{3},\theta)| = 1 \tag{5.2-7b}$$

Equation (5.2-7*a*) can be manipulated in the specific case at hand to yield

$$\frac{k \sin 3\theta}{2 + k^2 + k \cos 3\theta} = \tan\left(\frac{\pi}{2} - 2 \tan^{-1} \frac{(\omega\tau/3)(\alpha - 1)}{1 + \alpha(\omega\tau/3)^2}\right) \tag{5.2-8}$$

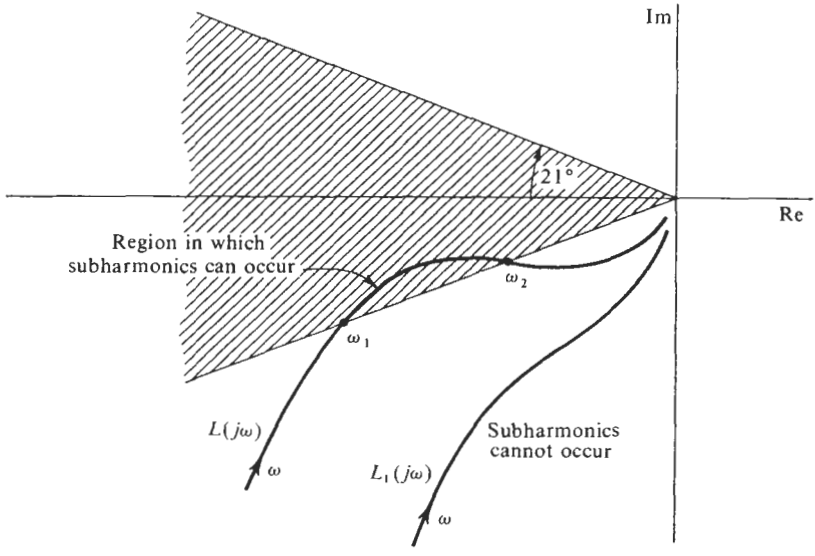

Figure 5.2-1 *The 21° rule for elimination of one-third-subharmonic generation in systems with a cubic nonlinearity. (Adapted from West, Ref. 23.)*

which is, in fact, a quadratic in k for fixed ω, θ. Similarly, Eq. (5.2-7*b*) can be manipulated to yield

$$A = \sqrt{\frac{4\omega}{9K}\frac{1 + (\alpha\omega\tau/3)^2}{[1 + (\omega\tau/3)^2]\sqrt{(2 + k^2 + k\cos 3\theta)^2 + (k \sin 3\theta)^2}}} \tag{5.2-9}$$

The last relationship required corresponds to Eq. (5.2-5). This gives three equations in the three unknowns, A, B, θ, provided that ω is held constant.

Insofar as the three equations arrived at are themselves particularly nonlinear, their closed-form solution is not sought. However, the desired solution can still be obtained. By picking values of θ in the range $0 \leq \theta \leq 120°$, the corresponding values of k are specified in terms of Eq. (5.2-8). Only positive real values of k are of interest. Next, Eq. (5.2-9)

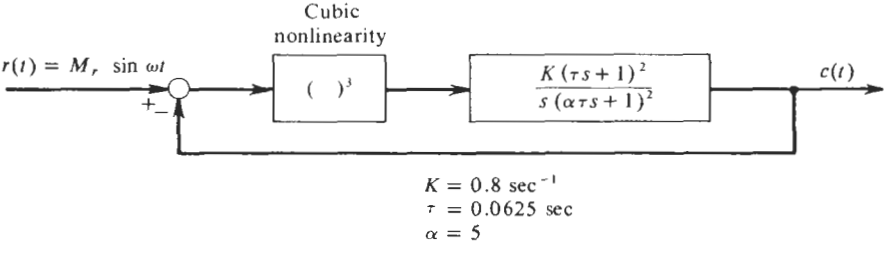

Figure 5.2-2 *Third-order system with cubic nonlinearity.*

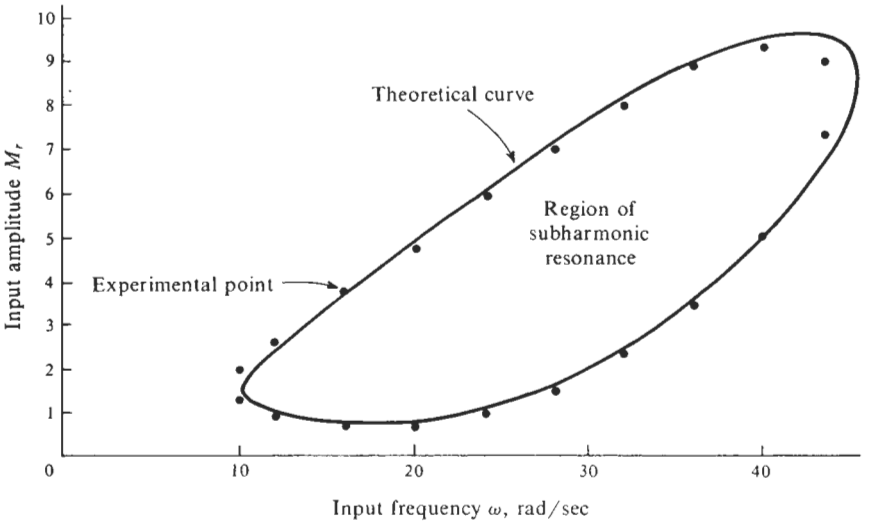

Figure 5.2-3 *Region of subharmonic resonance for example system.*

yields the values of A which correspond to the pairs of values (θ,k). Finally, the last equation is used to determine the corresponding M_r.

As ω is varied, the complete range of solutions is traversed. Theoretical results and excellent analog-computer verification are illustrated in Fig. 5.2-3. A typical input-output waveform pair is illustrated in Fig. 5.2-4*a*. The "resonance" is apparent. As the input amplitude is either increased or decreased, a point is reached at which the subharmonic resonance disappears. Figure 5.2-4*b* depicts the decay of the subharmonic mode due to a *slight* decrease in the input amplitude. Observe that the steady-state response beyond the subharmonic region, in this case at least, is imperceptible.

It is often stated, erroneously, that only odd harmonics can occur in systems containing an odd nonlinearity. This interesting error appears to be the consequence of one major aspect of approximation techniques, namely, you get *only* what you ask for. Thus, in the cubic nonlinearity system of Example 5.2-1, even subharmonics (of order one-half) were indeed observed during simulation; however, a *bias* was associated with the corresponding nonlinearity input. Unless this bias is specifically provided for in the model nonlinearity input waveform, approximation methods such as TSIDF analysis fail to predict the even subharmonic mode.

Finally, it is to be noted that the frequency domain criterion for avoiding subharmonics (i.e., 21° rule for systems with a cubic nonlinearity) is far more readily applied than detailed determination of the region in M_r, ω coordinates throughout which subharmonics can occur. In fact, analytic descriptions of the subharmonic TSIDFs for common nonlinearities are generally not available, although some have been obtained experimentally. For the

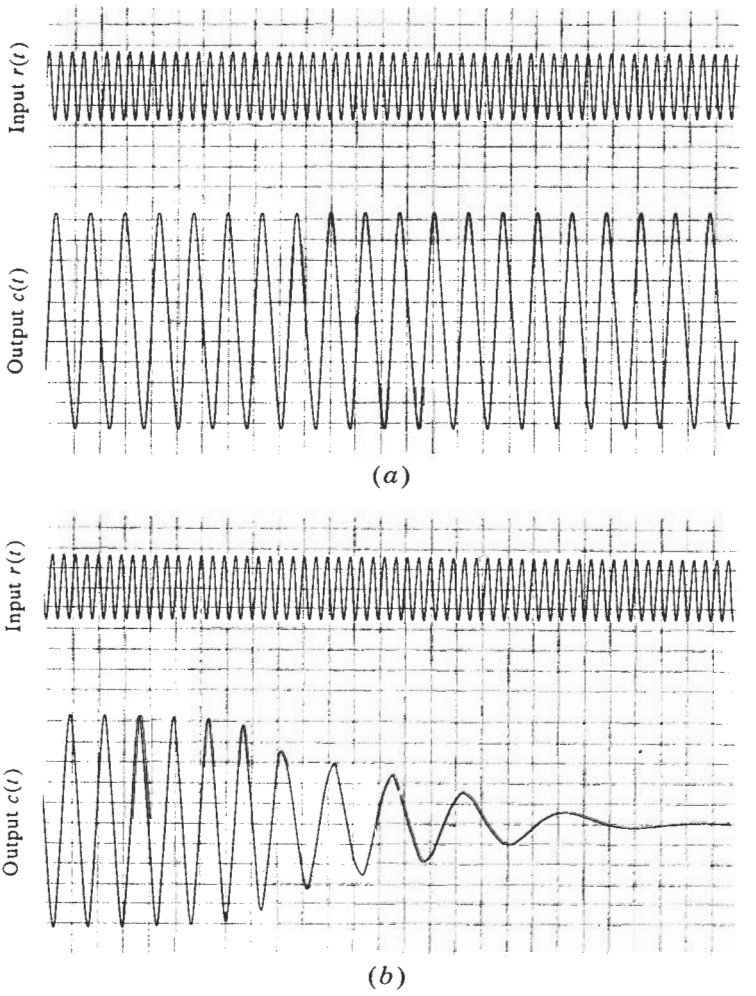

Figure 5.2-4 *(a) Illustration of subharmonic resonance. (b) Decay of a subharmonic mode.*

piecewise-linear limiter ($D = \delta = 1$), Douce and King (Ref. 6) have determined the bounds of the one-third-subharmonic TSIDF to be such that the condition for avoiding subharmonic resonance is as illustrated in Fig. 5.2-5. That for the ideal relay follows directly (cf. Prob. 5-8).

5.3 FREQUENCY RESPONSE COUNTEREXAMPLES

The DF calculation of frequency response in Chap. 3 is prefaced with a note of caution. It is stated there that certain non-limit-cycling systems break into a limit cycle oscillation when forced by a sinusoidal input (thus rendering invalid the DF calculation of frequency response), and also that certain

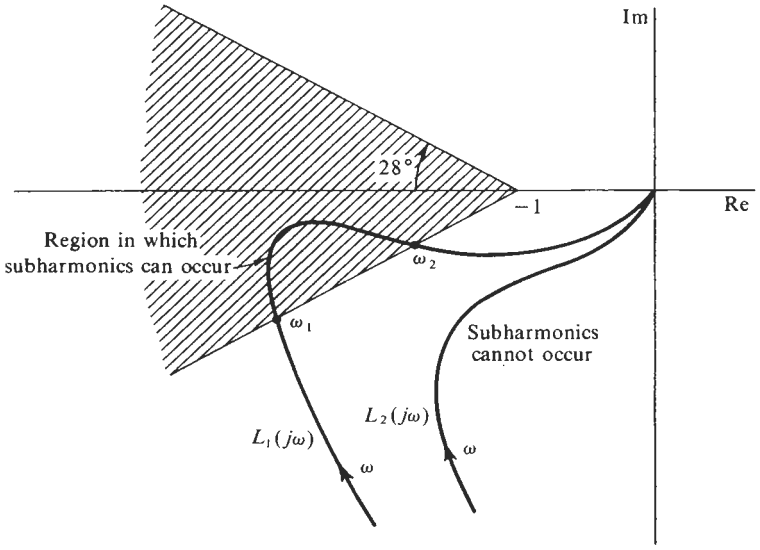

Figure 5.2-5 *The 28° rule for elimination of one-third-subharmonic generation in systems containing a limiter. (Adapted from Douce, Ref. 7.)*

limit cycling systems are quenched by the introduction of a sinusoidal input (thus permitting DF calculation of frequency response). In this section examples of each of the above phenomena are presented. The emphasis in presentation is on a physical interpretation of cause and effect. For further information the reader is referred to the interesting work of Gibson and Sridhar (Ref. 10), from which the following examples are drawn.

Example 5.3-1 *Limit cycle induction.* Consider the system of Fig. 5.3-1. This is a special case of Example 3.1-1 (that is, $\zeta = \omega_n = \delta = D = 1$), where it is shown by DF utilization that no limit cycle takes place when $K < 3.14$. For larger values of K a limit cycle of frequency $\omega_0 = 1$ exists.

Now set $K = 2$, so that $L(j1) = -1$, and apply an input $r = M_r \sin \omega t$. To test for

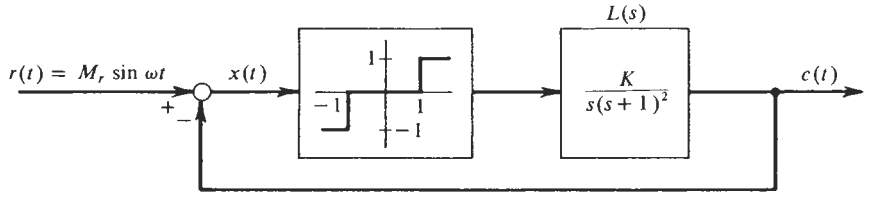

Figure 5.3-1 *An example of limit cycle induction.*

the possibility of a limit cycle, model the nonlinearity input according to

$$x = A \sin \omega t + B \sin t \tag{5.3-1}$$

where B is the limit cycle amplitude, should one exist. The requirement for a limit cycle in TSIDF terms is

$$N_B(A,B)L(j1) = -1$$

or simply,

$$N_B(A,B) = 1 \tag{5.3-2}$$

Whereas the DF for the relay with dead zone has a maximum value less than unity [such that no limit cycle can circulate according to the DF counterpart of Eq. (5.3-2)], the corresponding TSIDF can have values far in excess of unity. In particular, a range of A and B exist in which Eq. (5.3-2) is precisely satisfied; *a limit cycle can exist!*

The effect of an *externally* applied sinusoid has been to increase the (*internal*) loop gain to the point where an instability (i.e., limit cycle) can occur. To see the mechanism whereby the TSIDF gain can exceed unity, consider the value $A \approx 1.0$. The nonlinearity output never departs from zero, but input excursions carry right up to the discontinuities. Now a *very small* added signal (B) causes the output to jump to ± 1; hence the gain to the very small input under this circumstance is very large. This accounts for the behavior of the curve $\alpha = 1.0$ near the origin in Fig. D.3. Although not shown, there exists a continuous range of values $1.0 < \alpha < 1.3$ in which $N_B(A,B) \geq 1$. Therefore we conclude that all combinations of M_r and ω which result in $1.0 < A < 1.3$ are accompanied by an input-induced limit cycle.

Example 5.3-2 *Limit cycle quenching.* Consider the system of Fig. 5.3-2. This is a special case of Example 3.7-6 (that is, $\zeta = \omega_n = D = 1$), where it is noted that a limit cycle of frequency $\omega_0 = 1$ exists for all values of K.

Once again, set $K = 2$, apply an input $r = M_r \sin \omega t$, and model the system error signal according to Eq. (5.3-1). The condition for the limit cycle to continue is then satisfaction of Eq. (5.3-2). Figure D.1, a normalized plot of the ideal-relay TSIDF, illustrates that for *any* specified value of B, $N_B(A,B)$ decreases as A increases. It follows that there exists a value of A, which we denote $A_{\min}$, such that, for any value of A in the range $A_{\min} < A < \infty$, $N_B(A,B)$ is always less than unity, and no limit cycle can circulate.

$A_{\min}$ is readily calculated. In the region of its maximum value, $N_B(A,B)$ is given by Eq. (5.1-35), namely,

$$N_B(A,B) = \frac{8}{\pi^2 B} E\left(\frac{A}{B}\right) \qquad \frac{B}{A} > 1$$

$$= \frac{8}{\pi^2 A} xE(x)$$

where $x = A/B$. With the aid of the differential relationship

$$\frac{dE(x)}{dx} = \frac{1}{x}[E(x) - K(x)]$$

the value of x which maximizes $N_B(A,B)$, denoted $x_{\max}$, is found to satisfy

$$2E(x_{\max}) = K(x_{\max})$$

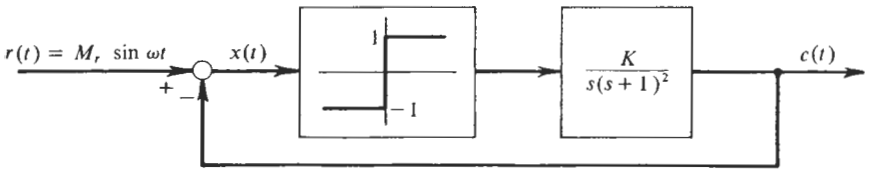

Figure 5.3-2 *An example of limit cycle quenching.*

Standard tables of the complete elliptic integrals can be consulted to yield that

$$x_{\max} \approx 0.909$$

at which point the maximum value of $N_B(A,B)$ is computed as

$$N_B(A,B)_{\max} = \frac{0.855}{A}$$

This results in the determination that $A_{\max} = 0.855$. Hence all combinations of M_r and ω for which $A > 0.855$ drop the loop gain at the limit cycle frequency to the point where the limit cycle is quenched (e.g., extinguished). These combinations are determined with DF theory, since there is now but one sinusoid with which to contend.

Circumstances under which a DF treatment of frequency response is insufficient can be deduced from the foregoing examples. Non-limit-cycling systems which can support a limit cycle at some values of loop gain (either higher or lower than the no-limit-cycle setting) must be checked by a TSIDF calculation to ensure the absence of a limit cycle. Limit cycling systems which can be quenched by either a raised or lowered loop gain should also be subject to TSIDF calculation to determine the range in which a frequency response exists. This phenomenon, called *signal stabilization*, is treated in more detail in Chap. 6.

5.4 MULTIPLE LIMIT CYCLES

Nonlinear systems often exhibit more than a single stable limit cycle. In such multiple limit cycle systems the possibilities exist that either one limit cycle predominates, several limit cycles occur one at a time, or several limit cycles occur simultaneously. A TSIDF argument is required for determination of the circumstances leading to the first of these alternatives.

Consider the relay system of Fig. 5.4-1*a* for which DF theory tells us that the limit cycles at frequencies ω_A (higher) and ω_B (lower) are stable. If the higher-frequency limit cycle is excited, the following relationship must hold:

$$N_A(A,B)\,|L(j\omega_A)| = 1 \qquad (5.4\text{-}1)$$

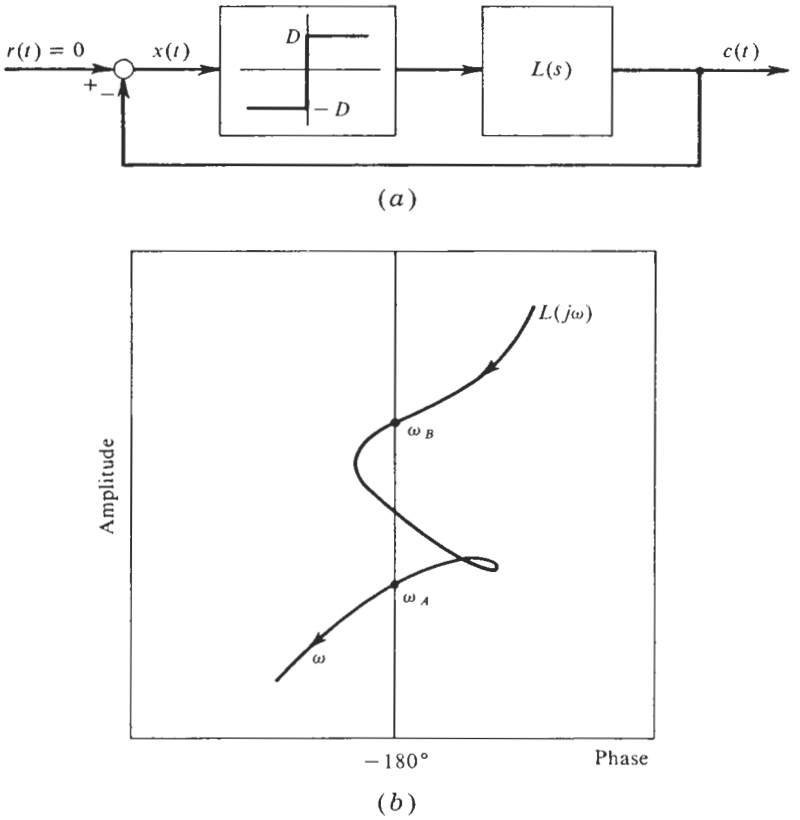

Figure 5.4-1 *(a) Multiple limit cycle system. (b) Corresponding amplitude-phase plot.*

where A is the limit cycle amplitude and $B = 0$. Now, using as a model for the nonlinearity input

$$x = A \sin \omega_A t + B \sin \omega_B t \tag{5.4-2}$$

where $B \ll A$, the TSIDF is employed to determine the nature of stability of the perturbed low-frequency limit cycle mode. The procedure is quite direct. Use of Eq. (5.1-20) enables rewriting Eq. (5.4-1) in the form

$$N_B(A,B)\,|L(j\omega_B)| = \frac{1}{2}\left|\frac{L(j\omega_B)}{L(j\omega_A)}\right| \tag{5.4-3}$$

from which it is deduced that the perturbed low-frequency mode is *unstable* if

$$\left|\frac{L(j\omega_B)}{L(j\omega_A)}\right| > 2 \tag{5.4-4}$$

that is, the oscillation grows. Hence, when Eq. (5.4-4) is satisfied, the high-frequency limit cycle alone is *not* a stable systematic mode. Otherwise it is.

Now apply the same argument to test the reverse situation. This almost always shows the perturbed high-frequency mode to be *stable* in the presence of a low-frequency limit cycle since the condition $|L(j\omega_A)|L(j\omega_B)| > 2$ is rare indeed. In those circumstances where this mode is *unstable*, the linear element's frequency locus is highly resonant in the vicinity of ω_A. Nonlinearity output harmonic content near ω_A is consequently not negligible, and as a result, the TSIDF linearization is inappropriate. A somewhat different argument is required to ascertain conditions of stability. To facilitate analysis, the case where only the fundamental and the harmonic component nearest the higher-frequency oscillation mode is of significant amplitude can be treated. This is the approach taken in Ref. 1.

5.5 INCREMENTAL-INPUT DESCRIBING FUNCTION

A special case of the TSIDF occurs when the amplitude of one nonlinearity input sinusoid is much smaller than the amplitude of the other.[1] Under this circumstance, a simple closed-form solution exists for the nonlinearity gain to the small-amplitude input component; it is called the *incremental-input describing function*. This particular describing function is of considerable interest. It has application to the study of oscillation stability (including stability of forced sinusoidal response and limit cycle stability), and importantly, it is an excellent approximation to the TSIDF in the case of widely differing input amplitudes. Following the nomenclature used by Bonenn (Ref. 4), we consider separately the cases of synchronous (i.e., identical frequency) inputs and nonsynchronous (i.e., different frequency) inputs.

DERIVATION OF THE INCREMENTAL-INPUT DESCRIBING FUNCTION

Synchronous inputs Let the two sinusoidal inputs to a static nonlinearity be given by

$$x = A \sin \omega t + \epsilon \sin (\omega t + \theta) \tag{5.5-1}$$

where the second term represents the *incremental input*, that is,

$$\frac{\epsilon}{A} \ll 1 \tag{5.5-2}$$

[1] The content of this section can be viewed as a direct result of TSIDF expansion in a power series (Sec. 5.1). Rather than simply setting B to zero in Eqs. (5.1-43*a*) and (5.1-44*a*), a brief and more direct derivation of the describing functions of interest is presented here.

Expanding Eq. (5.5-1) and regrouping terms, x can be put in the form

$$x = (A + \epsilon \cos\theta) \sin \omega t + (\epsilon \sin\theta) \cos \omega t$$

$$= \sqrt{(A + \epsilon \cos\theta)^2 + (\epsilon \sin\theta)^2} \sin\left(\omega t + \tan^{-1} \frac{\epsilon \sin\theta}{A + \epsilon \cos\theta}\right) \quad (5.5\text{-}3)$$

Using the relative amplitude constraint [Eq. (5.5-2)], the expressions for input magnitude and phase can be further simplified. Dropping second- and higher-order terms in ϵ/A, we have

$$\sqrt{(A + \epsilon \cos\theta)^2 + (\epsilon \sin\theta)^2} \approx A + \epsilon \cos\theta \quad (5.5\text{-}4)$$

and

$$\tan^{-1} \frac{\epsilon \sin\theta}{A + \epsilon \cos\theta} \approx \frac{\epsilon}{A} \sin\theta \quad (5.5\text{-}5)$$

Hence Eq. (5.5-1) can be written in the alternative form

$$x \approx (A + \epsilon \cos\theta) \sin\left(\omega t + \frac{\epsilon}{A} \sin\theta\right) \quad (5.5\text{-}6)$$

If $N(A) = n_p(A) + jn_q(A)$ is the DF for the nonlinearity, and has a continuous first derivative with respect to A, the output is (prime denoting differentiation with respect to A)

$$\text{Output} \approx (A + \epsilon \cos\theta)[n_p(A + \epsilon \cos\theta)] \sin\left(\omega t + \frac{\epsilon}{A} \sin\theta\right)$$

$$+ (A + \epsilon \cos\theta)[n_q(A + \epsilon \cos\theta)] \cos\left(\omega t + \frac{\epsilon}{A} \sin\theta\right)$$

$$\approx (A + \epsilon \cos\theta)[n_p(A) + \epsilon \cos\theta\, n_p'(A)]\left(\sin \omega t + \frac{\epsilon}{A} \sin\theta \cos \omega t\right)$$

$$+ (A + \epsilon \cos\theta)[n_q(A) + \epsilon \cos\theta\, n_q'(A)]\left(\cos \omega t - \frac{\epsilon}{A} \sin\theta \sin \omega t\right)$$

$$\approx A[n_p(A) \sin \omega t + n_q(A) \cos \omega t]$$

$$+ \epsilon[n_p(A) \sin(\omega t + \theta) + n_q(A) \cos(\omega t + \theta)$$

$$+ A \cos\theta\,(n_p'(A) \sin \omega t + n_q'(A) \cos \omega t)] \quad (5.5\text{-}7)$$

where again only first-order terms in ϵ/A have been retained. Defining the incremental-input describing function as the complex ratio of output terms due to ϵ divided by the corresponding input term, we finally arrive at the

desired result,

$$N_i(A,\theta) = \text{incremental-input describing function}$$

$$= \frac{\epsilon[n_p(A)e^{j(\omega t+\theta)} + n_q(A)e^{j(\omega t+\theta+\pi/2)} + A\cos\theta\,(n'_p(A)e^{j\omega t} + n'_q(A)e^{j(\omega t+\pi/2)})]}{\epsilon\, e^{j(\omega t+\theta)}}$$

$$= n_p(A) + jn_q(A) + A[n'_p(A) + jn'_q(A)]\cos\theta\, e^{-j\theta}$$

$$= N(A) + AN'(A)\cos\theta\, e^{-j\theta} \tag{5.5-8}$$

Observe that the incremental-input describing function is independent of ϵ and is derivable directly from the ordinary DF for the nonlinearity. By rearranging the θ dependence of $N_i(A,\theta)$, one may show that

$$N_i(A,\theta) = N(A) + \frac{AN'(A)}{2}(1 + e^{-j2\theta}) \tag{5.5-9}$$

in which form it is evident that, for fixed A, the tip of the vector $N_i(A,\theta)$ traces out a circle in the polar plane (see Fig. 5.5-1).

Nonsynchronous inputs The nonlinearity input is now taken as

$$x = A\sin\omega t + \epsilon\sin\gamma\omega t \tag{5.5-10}$$

where the frequency ratio γ is *irrational*, and the condition expressed by Eq. (5.5-2) still holds. The phase angle θ has been discarded since x now possesses an aperiodic waveform. In fact, by considering θ to be a uniformly distributed random variable, one can derive the incremental-input describing function pertinent to the present case simply by averaging $N_i(A,\theta)$ of the synchronous case [Eq. (5.5-9)] with respect to θ. The result, independent of θ, is given by (Ref. 4)

$$N_i(A) = N(A) + \frac{AN'(A)}{2} \tag{5.5-11}$$

This is precisely the relationship arrived at by setting B to zero in Eq. (5.1-44*a*). That is,

$$N_i(A) = W_0(A) \tag{5.5-12}$$

where $W_0(A)$ is the first term in the expansion of $N_B(A,B)$ in powers of B.

APPLICATION TO JUMP RESONANCE PHENOMENA

A natural application for the synchronous incremental-input describing function lies in the study of jump resonance phenomena (Sec. 3.3). For the nonlinear system of Fig. 5.5-2*a*, the possibility of jump resonance can be studied in terms of the stability of a sinusoidal perturbation of frequency ω

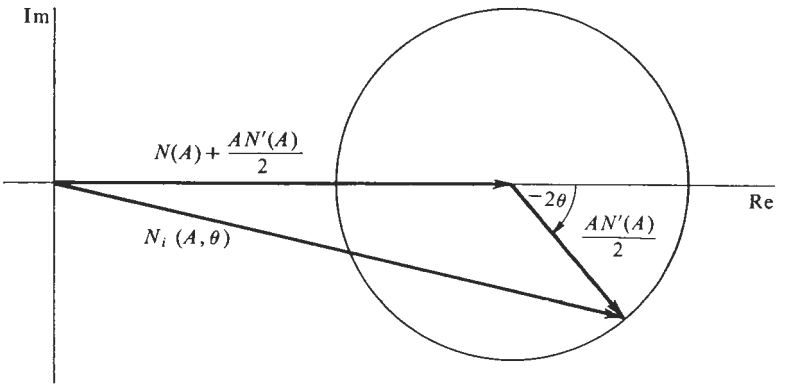

Figure 5.5-1 *Complex representation of $N_i(A,\theta)$ for synchronous inputs. Illustrated for the case where $N(A)$ is real.*

about a steady-state forced oscillation at the same frequency. The characteristic equation of the system seen by such a perturbation is (Fig. 5.5-2*b*)

$$1 + N_i(A,\theta)L(j\omega) = 0 \tag{5.5-13}$$

or

$$L(j\omega) = -\frac{1}{N_i(A,\theta)} \tag{5.5-14}$$

For fixed A, the quantity $-1/N_i(A,\theta)$ plays the role of a *stability point*, or more properly, a *stability curve*, since θ can take on any value from 0 to 2π radians. Whereas with the ordinary DF an instability (limit cycle) is indicated when the locus $L(j\omega)$ passes through the *point* $-1/N(A)$, now an instability (jump resonance) is indicated when the locus $L(j\omega)$ passes through any portion of the *curve* $-1/N_i(A,\theta)$. This new point of view regarding the

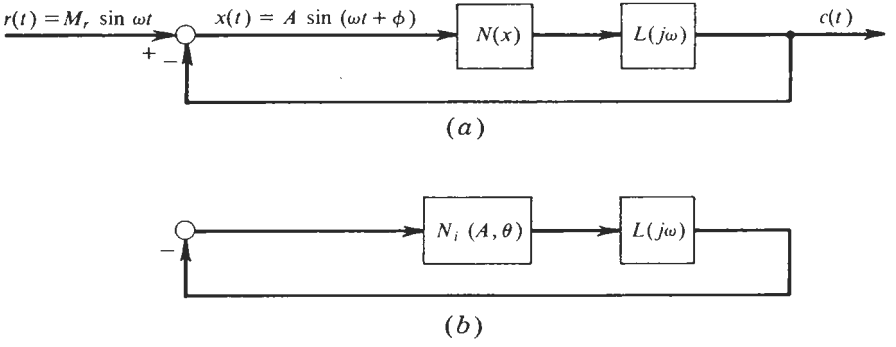

Figure 5.5-2 *(a) Nonlinear system. (b) Corresponding incremental system.*

jump resonance phenomenon is easily demonstrated as being equivalent to that presented earlier, in Sec. 3.3.

Example 5.5-1 Derive the equations for the contours in the polar plane along which jump resonance can occur.

Expressing $L(j\omega)$ in the form $U(\omega) + jV(\omega)$, Eq. (5.5-13) can be written as

$$1 + \left[N(A) + \frac{AN'(A)}{2}(1 + e^{-j2\theta})\right][U(\omega) + jV(\omega)] = 0 \tag{5.5-15}$$

Equating the real and imaginary parts on each side gives

$$1 + \left[N(A) + \frac{AN'(A)}{2}(1 + \cos 2\theta)\right] U(\omega) + \left[\frac{AN'(A)}{2}\sin 2\theta\right] V(\omega) = 0$$

$$\left[N(A) + \frac{AN'(A)}{2}(1 + \cos 2\theta)\right] V(\omega) - \left[\frac{AN'(A)}{2}\sin 2\theta\right] U(\omega) = 0$$

Eliminating θ between these equations and manipulating yields

$$\left[U(\omega) + \frac{1}{2}\left(\frac{1}{N(A)} + \frac{1}{N(A) + AN'(A)}\right)\right]^2 + V(\omega)^2 = \left[\frac{AN'(A)}{2N(A)[N(A) + AN'(A)]}\right]^2 \tag{5.5-16}$$

Geometrically interpreted, the contours of constant A are circles, with center coordinates $(-\frac{1}{2}\{1/N(A) + 1/[N(A) + AN'(A)]\}, 0)$ and radii $|AN'(A)/2N(A)[N(A) + AN'(A)]|$.

It is readily seen that Eqs. (5.5-16) and (3.3-12) are identical. This establishes the equivalence of both ways of viewing the condition for jump resonance. The reader is referred to Sec. 3.3 for further discussion of jump resonance phenomena.

APPLICATION TO TRANSIENT OSCILLATIONS

This section is concerned with the relative stability of small perturbations about steady-state oscillations in nonlinear systems. The systems are assumed describable by equations of the type

$$Q(s)x + P(s)y(x,\dot{x}) = 0 \tag{5.5-17}$$

where $s = d/dt$, and $P(s)$ and $Q(s)$ are polynomials in s. The differential operator corresponding to the system linear elements' transfer function is $L(s) = P(s)/Q(s)$, and the nonlinearity output is characterized by $y(x,\dot{x})$.

For the study of relative stability, the test signal applied to Eq. (5.5-17) is chosen in the form[1]

$$x(t) = Ae^{j\omega_0 t} + \epsilon e^{\sigma t}e^{j(\omega_0 t + \theta)} \tag{5.5-18}$$

[1] By convention the *real* test signal is understood to be the imaginary part of this *complex* expression. The derivation closely follows Bonenn (Ref. 4).

where ϵ is an arbitrary but small parameter. Substituting for $x(t)$ in Eq. (5.5-17) yields, after making the describing function approximation,

$$Q(s)(Ae^{j\omega_0 t} + \epsilon e^{\sigma t}e^{j(\omega_0 t+\theta)}) + P(s)(AN(A)e^{j\omega_0 t} + \epsilon N_i(A,\theta)e^{\sigma t}e^{j(\omega_0 t+\theta)}) = 0 \quad (5.5\text{-}19)$$

The dominant terms in this equation, of order A, represent the steady-state oscillation and sum exactly to zero. For the remaining perturbation terms, application of the differential-operator rules (Ref. 19),

$$L(s)[e^{\sigma t}f(t)] = e^{\sigma t}L(s+\sigma)[f(t)] \quad (5.5\text{-}20)$$

$$L(s)[e^{j\omega t}] = e^{j\omega t}L(j\omega) \quad (5.5\text{-}21)$$

yields

$$\epsilon e^{\sigma t}e^{j(\omega_0 t+\theta)}[Q(\sigma + j\omega_0) + N_i(A,\theta)P(\sigma + j\omega_0)] = 0 \quad (5.5\text{-}22)$$

To satisfy equality with zero requires that the term in brackets vanishes; the perturbation signal itself is arbitrary. Dividing this term by $Q(\sigma + j\omega_0)$ gives, as the characteristic equation of the perturbed system,

$$1 + N_i(A,\theta)L(\sigma + j\omega_0) = 0 \quad (5.5\text{-}23)$$

where ω_0 is the steady-state oscillation frequency, and σ is the damping factor of interest. Equation (5.5-23) is a generalization of Eq. (5.5-13), the latter implicitly assuming $\sigma = 0$. The transition from Eq. (5.5-13) to (5.5-23) is analogous to the transition from stability determination by frequency methods to stability characterization in terms of poles and zeros. Of course, it is assumed in writing Eq. (5.5-23) that $N_i(A,\theta)$ is the appropriate gain to associate with an incremental input $\epsilon \exp(\sigma t) \sin \omega_0 t$. For σ sufficiently close to zero, this approximation is certainly valid. The nature of the approximation is identical with that made in Chap. 4, where $N(A)$ is used to characterize the nonlinearity in response to a sinusoid of slowly varying amplitude and frequency. The point of view adopted here, however, is quite different from that in Chap. 4.

A graphical procedure is employed to extract the desired solution of Eq. (5.5-23). It is best demonstrated by an example.

Example 5.5-2 Calculate the damping factor associated with limit cycle perturbations in the system of Fig. 5.5-3.

Recall of the DF for a preload nonlinearity enables writing the steady-state limit cycle equation as

$$\left(\frac{4}{\pi A} + 1\right)\frac{1}{j\omega_0(j\omega_0 + 1)^2} = -1$$

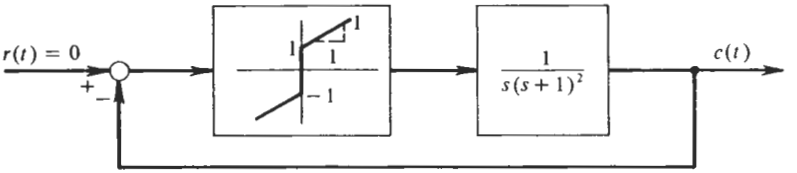

Figure 5.5-3 Limit cycling system.

This equation is satisfied by $\omega_0 = 1$ and $A = 4/\pi$. Now, from Eq. (5.5-9), the synchronous incremental-input describing function for the preload nonlinearity is

$$N_i(A,\theta) = \frac{4}{\pi A} + 1 + \frac{A}{2}\left(-\frac{4}{\pi A^2}\right)(1 + e^{-j2\theta})$$

$$= \frac{3}{2} - \frac{1}{2}e^{-j2\theta}$$

To facilitate solution, Eq. (5.5-23) is best put in the form

$$-N_i(A,\theta) = \frac{1}{L(\sigma + j\omega_0)}$$

Writing this equation in terms of the present problem gives the following complex relationship:

$$-\frac{3}{2} + \frac{1}{2}e^{-j2\theta} = (\sigma + j)(\sigma + 1 + j)^2$$

Since the left-hand side is a function of θ only, and the right-hand side is a function of σ only, this set of two equations in two unknowns can be readily solved by plotting each side as a function of the pertinent variable and determining intersections of the resultant loci. This is illustrated in Fig. 5.5-4, where we find the solutions $\sigma = 0$ and $\sigma \approx -0.1$. Notably, the quasi-static solution of Chap. 4 also leads to the value $\sigma = -0.1$.

It can be seen in general that at $\omega = \omega_0$, Eq. (5.5-23) has two solutions for σ. One of these always occurs at $\sigma = 0$, and corresponds to the steady-state change in the limit cycle. The other, at negative σ for stable limit cycles, corresponds to the time constant of the limit cycle transient. It is the measure of relative stability which we seek. The analog-computer result shown in Fig. 5.5-4 attests to the accuracy of this calculation, providing an experimental time constant of about 10 sec (that is, $\sigma_{\text{exper}} \approx -0.1$ sec^{-1}).

APPLICATION TO TSIDF APPROXIMATION

An important use for the nonsynchronous incremental-input describing function occurs in TSIDF approximation for the case of widely differing input amplitudes. The approximating relationships are, from Eq. (5.5-7),

$$\tilde{N}_A(A,B) = N(A) \tag{5.5-24}$$

and from Eq. (5.5-8),

$$\tilde{N}_B(A,B) = N_i(A) \tag{5.5-25}$$

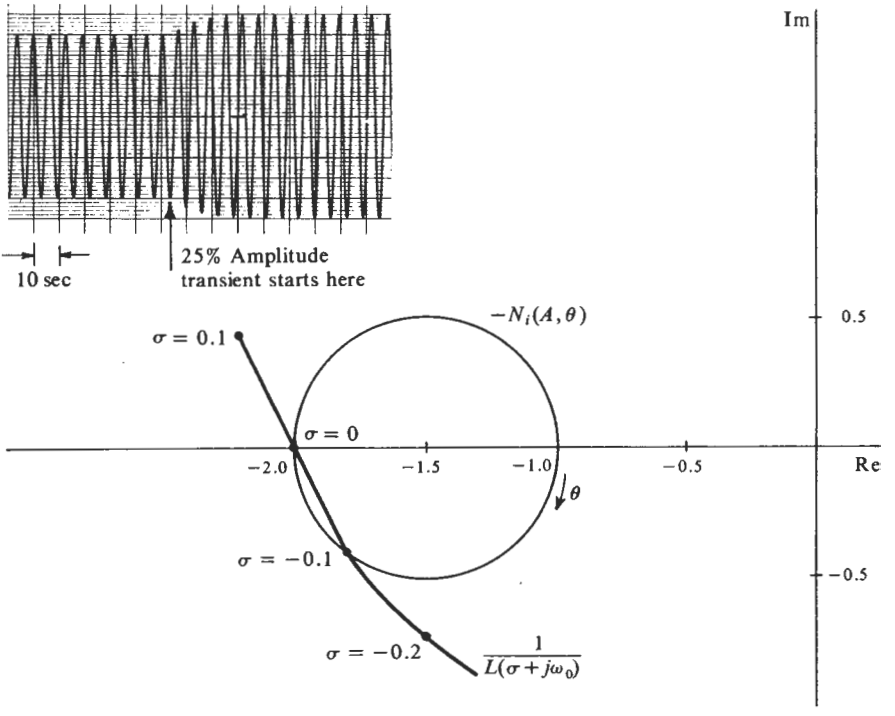

Figure 5.5-4 *Graphical solution for the limit cycle transient damping factor. Insert shows analog-computer results*

where a tilde denotes the approximation. The requirement is that B be sufficiently small for these approximations to hold. For the majority of nonlinear characteristics, this implies an upper bound on the ratio B/A. For nonlinear characteristics periodic in x (such as the harmonic nonlinearity $y = \sin mx$), this implies a limit on the absolute value of B.

Example 5.5-3 Determine the requirement on B under which the harmonic nonlinearity TSIDFs can be approximated to within 10 percent accuracy by the DF and incremental-input describing function [Eqs. (5.5-24) and (5.5-25)].

For the harmonic nonlinearity $y = \sin mx$, it is readily demonstrated (see Prob. 5-3) that the exact TSIDFs are

$$N_A(A,B) = \frac{2}{A} J_0(mB)J_1(mA) \tag{5.5-26}$$

$$N_B(A,B) = \frac{2}{B} J_0(mA)J_1(mB) \tag{5.5-27}$$

According to the proposed approximations, it follows from Eq. (2.3-23) that

$$\tilde{N}_A(A,B) = \frac{2}{A} J_1(mA) \tag{5.5-28}$$

and from Eq. (5.5-11),

$$\begin{aligned}\tilde{N}_B(A,B) &= \frac{2}{A} J_1(mA) + \frac{A}{2} \frac{d}{dA}\left[\frac{2}{A} J_1(mA)\right] \\ &= mJ_0(mA)\end{aligned} \tag{5.5-29}$$

Comparing Eqs. (5.5-26) and (5.5-28) yields that the exact and approximating TSIDFs differ by the factor $J_0(mB)$. This factor is bounded by 1.0 and 0.9 for mB in the range $|mB| < 0.65$. Now comparing Eqs. (5.5-27) and (5.5-29), we see that the factor of difference is $2J_1(mB)/mB$. This factor is bounded by 1.0 and 0.9 for mB in the range $|mB| < 0.89$. Hence the requirement on B is

$$|mB| < 0.65$$

which is, indeed, independent of A, as noted previously.

The relative ease with which the TSIDF approximation can be calculated certainly promotes its use as an analytical tool. Applications for this particular form of linearization are both diverse and numerous. A typical application is illustrated below.

Example 5.5-4 An optical-beam-riding antitank missile has its position control loop closed by a human operator. The on-off rate control loop employs a 400-cps carrier rate gyro feedback signal and associated amplification, demodulation, and compensation, as shown in Fig. 5.5-5. Assume that the airframe dynamics from δ to ψ are characterized by the transfer function

$$\frac{\psi}{\delta}(s) = \frac{50(s+1)}{s(s^2+2s+25)}$$

It is found that the in-flight missile trajectory oscillates about the optical tracker-target line of sight, producing a signal $e = 25 \sin 6t$ volts. Find the amplitude of missile control-surface deflection due to a 1-volt demodulator output noise at the carrier frequency.

The nonlinearity input is modeled according to

$$x \approx A \sin 6t + B \sin 2{,}512t$$

We first have to calculate the amplitude A of the low-frequency nonlinearity input component. This is given by the solution to the relationship

$$A = \left| \frac{\dfrac{0.1s+1}{s+1} 25}{1 + \dfrac{0.1s+1}{s+1} N(A) \dfrac{50(s+1)}{s^2+2s+25}} \right|_{s=j6}$$

where the approximation to $N_A(A,B)$ is the DF for the on-off element with dead zone

$$\tilde{N}_A(A,B) = \frac{4}{\pi A} \sqrt{1 - \left(\frac{0.5}{A}\right)^2}$$

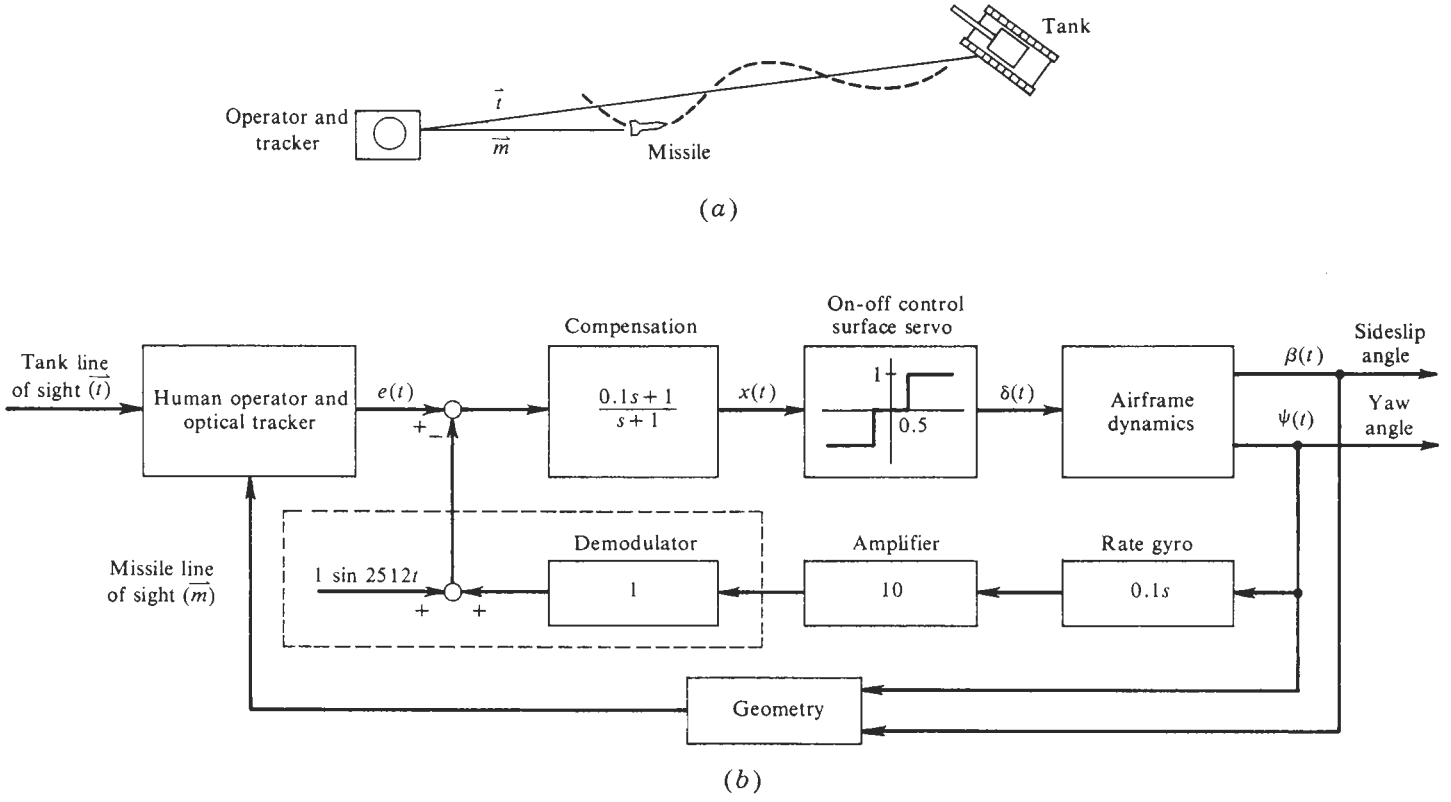

Figure 5.5-5 *(a) Antitank missile problem geometry. (b) Control-system configuration.*

The solution to these equations is readily found to be $A = 2.5$. Next the incremental-input describing function gain must be calculated in approximation to $N_B(A,B)$.

$$\tilde{N}_B(A,B) = \frac{4}{\pi A}\sqrt{1 - \left(\frac{0.5}{A}\right)^2} + \frac{A}{2}\frac{d}{dA}\left[\frac{4}{\pi A}\sqrt{1 - \left(\frac{0.5}{A}\right)^2}\right]$$

$$= \frac{2}{\pi A}\sqrt{1 - \left(\frac{0.5}{A}\right)^2} + \frac{0.5}{\pi A^3\sqrt{1 - (0.5/A)^2}}$$

This expression is evaluated at the appropriate value for A.

$$\tilde{N}_B(A,B)\Big|_{A=2.5} = 0.26$$

The system seen by the sinusoidal noise voltage has thus been linearized. Neglecting the small fed-back high-frequency signal, the required control-surface noise-deflection amplitude δ_n is calculated as

$$\delta_n \approx 1 \times \left|\frac{j(0.1)(2,512) + 1}{j2,512 + 1}\right| \times 0.26 = 0.026 \text{ radian}$$

This result is particularly interesting in view of the fact that δ_n would be zero if e were zero. Nonlinearity modification by one input as seen by another input is a phenomenon which can be put to practical use. We shall meet it repeatedly in the remainder of the text.

It is of some interest to check the accuracy of the TSIDF approximation employed. Using earlier notation, we have $A \approx 2.5$, $B \approx 0.1$. Entering Fig. D.1 at the curve labeled $A/\delta = 5$ (which is not shown, but interpolation is sufficient for our purposes here), we find at $B/\delta = 0.2$ the value $N_B(A,B)\delta/D \approx 0.13$, or $N_B(A,B) \approx 0.26$. This is certainly an excellent check on our approximation. It is also possible to check the value of $N_A(A,B)$, although to use the above-mentioned figure, we must employ Eq. (5.1-32). Hence, in place of $N_A(A,B)$, we choose to evaluate $N_B(B,A)$. This places us just below the curve labeled $A/\delta = 0$ at the abscissa value $B/\delta = 5$. The result is the determination that $N_A(A,B) \approx 0.50$. This justifies the use of $\tilde{N}_A(A,B)$, which also has the value 0.50 at $A = 2.5$.

5.6 ADDITIONAL TSIDF APPLICATIONS

By straightforward describing function technique one may use the TSIDF to study the complete forced harmonic response of a limit cycling system and, similarly, the response of a non-limit-cycling system to two simultaneously applied sinusoids. Interpretation of the nonlinearity input signal component parts is evident in each of these cases.

A conditionally stable system is one in which the linear elements' frequency locus has some frequency region displaying greater than 180° phase lag and, simultaneously, a gain in excess of unity. If, for example, such a system contains a limiter, a limit cycle can exist, following a suitable input transient. DF application can determine the limit cycle amplitude and frequency, but not the amplitudes and frequencies of input sinusoids which excite the limit cycle. TSIDF theory is readily applied here (Ref. 22).

Other TSIDF applications include the consideration of harmonic content in loop oscillations (i.e., DF correction term) and the analysis of systems with two nonlinearities separated by filters which insufficiently attenuate harmonics so that ordinary DF application is inaccurate (Ref. 23).

It must be remarked that, in general, TSIDF calculation for harmonically related input sinusoids is laborious. Where alternative methods of analysis obviate the need for this calculation, they may well be preferred. On the other hand, TSIDF calculation in the case of non-harmonically-related input sinusoids is quite easily accomplished. Calculation of the incremental-input describing function proceeds with no difficulty whatever. Once calculated, the employment of various TSIDFs for nonlinear-system study proceeds with the simplicity characteristic of describing function techniques.

REFERENCES

1. Amsler, B. E., and R. E. Gorozdos: On the Analysis of Bi-stable Control Systems, *IRE Trans. Autom. Control*, vol. AC-4 (December, 1959).
2. Bennett, W. R.: New Results in the Calculation of Modulation Products, *Bell System Tech. J.*, vol. 12 (1933), pp. 228–243.
3. Bonenn, Z.: Stability of Forced Oscillations in Nonlinear Feedback Systems, *IRE Trans. Autom. Control*, vol. AC-3 (December, 1958), pp. 109–111.
4. Bonenn, Z.: Relative Stability of Oscillations in Non-linear Control Systems, *Proc. IFAC*, Basel, Switzerland (August, 1963), p. 214/1–4.
5. Courant, R., and D. Hilbert: "Methods of Mathematical Physics," Interscience Publishers, Inc., New York, 1953, vol. 1, p. 475.
6. Douce, J. L., and R. E. King: Instability of a Nonlinear Conditionally Stable System Subjected to a Sinusoidal Input, *Trans. AIEE*, pt. II, *Appl. Ind.* (January, 1959), pp. 665–670.
7. Douce, J. L.: Discussion of a paper by Ogata, *Trans. ASME*, vol. 80, no. 8 (November, 1958), p. 1808.
8. Elgerd, O. I.: High-frequency Signal Injection: A Means of Changing the Transfer Characteristics of Nonlinear Elements, WESCON, 1962.
9. Gibson, J. E.: "Nonlinear Automatic Control," McGraw-Hill Book Company, New York, 1963.
10. Gibson, J. E., and R. Sridhar: A New Dual-input Describing Function and an Application to the Stability of Forced Oscillations, *Trans. AIEE*, pt. II, *Appl. Ind.* (May, 1963), pp. 65–70.
11. Hayashi, C.: "Nonlinear Oscillations in Physical Systems," McGraw-Hill Book Company, New York, 1964.
12. Huey, R. M., O. Pawloff, and T. Glucharoff: Extension of the Dual-input Describing-function Technique to Systems Containing Reactive Nonlinearity, *J. IEE*, London, vol. C-107 (June, 1960), pp. 334–341.
13. Jaffe, R. C.: Causal and Statistical Analyses of Dithered Systems Containing Three-level Quantizers, M.S. thesis, Massachusetts Institute of Technology, Cambridge, Mass., August, 1959.
14. Kalb, R. M., and W. R. Bennett: Ferromagnetic Distortion of a Two-frequency Wave, *Bell System Tech. J.*, vol. 14 (1935), pp. 322–359.

15. Ludeke, C. A.: The Generation and Extinction of Subharmonics, *Proc. Symp. Nonlinear Circuit Analysis*, vol. 2 (April, 1953), Polytechnic Institute of Brooklyn, New York.
16. MacColl, L. A.: "Fundamental Theory of Servomechanisms," D. Van Nostrand Company, Inc., Princeton, N.J., 1945.
17. Oldenburger, R., and R. C. Boyer: Effects of Extra Sinusoidal Inputs to Nonlinear Systems, *Trans. ASME, J. Basic Eng.* (December, 1962), pp. 559–570.
18. Oldenburger, R., and R. Nicholls: Stability of Subharmonic Oscillations in Nonlinear Systems, *Proc. JACC*, Minneapolis, Minn. (June, 1963), pp. 675–680.
19. Piaggio, H. T. H.: "Differential Equations," G. Bell & Sons, Ltd., London, 1946, p. 32.
20. Rice, S. O.: Mathematical Analysis of Random Noise, *Bell System Tech. J.*, vol. 24, pt. IV (1945), pp. 109–156.
21. West, J. C., and J. L. Douce: The Mechanism of Sub-harmonic Generation in a Feedback System, *J. IEE*, London, paper 1693 M, vol. B-102 (July, 1955), pp. 569–574.
22. West, J. C., J. L. Douce, and R. K. Livesley: The Dual Input Describing Function and Its Use in the Analysis of Non-linear Feedback Systems, *J. IEE*, London, vol. B-103 (July, 1956), pp. 463–474.
23. West, J. C.: "Analytical Techniques for Non-linear Control Systems," D. Van Nostrand Company, Inc., Princeton, N.J., 1960.

PROBLEMS

5-1. Calculate the TSIDFs in the cases of harmonically- and nonharmonically-related input sinusoids for the polynomial hard-spring characteristic given by

$$y = x + 0.3x^3$$

5-2. By employing the method of double Fourier series expansion, show that, for the half-wave linear rectifier,

$$y = \begin{cases} x & x \geq 0 \\ 0 & x < 0 \end{cases}$$

the first three output Fourier coefficients are (Ref. 2)

$$P_{00} = \frac{4A}{\pi^2}[2E(k) - (1 - k^2)K(k)]$$

$$P_{01} = \frac{kA}{2}$$

$$P_{10} = \frac{A}{2}$$

5-3. Demonstrate that for the nonlinearity

$$y = \sin mx$$

the function $Y(ju)$ can be obtained in the form

$$Y(ju) = \frac{\pi}{j}[\delta(u - m) - \delta(u + m)]$$

and hence that the TSIDFs are given by

$$N_B(A,B) = \frac{2}{B} J_0(mA)J_1(mB)$$

$$N_A(A,B) = \frac{2}{A} J_0(mB)J_1(mA)$$

[*Hint:* Use the relationship

$$\frac{1}{\pi} \lim_{\sigma \to 0} \frac{\sigma}{\sigma^2 + \alpha^2} = \delta(\alpha)$$

where $\delta(\alpha)$ denotes the unit-impulse function of argument α.]

5-4. Derive Eqs. (5.1-44*a*) to (5.1-44*c*). Use the result to evaluate the TSIDFs for an odd square-law nonlinearity, $y = x|x|$.

5-5. Compute the approximate TSIDFs for an ideal relay. According to the exact TSIDF expressions, what is the range of validity of the approximation?

5-6. What is the upper limit on input frequency which you would recommend for the system of Fig. 5-1 such that one-third subharmonics are not to occur? Design a linear compensator to be located at station y such that *no* one-third subharmonics can occur.

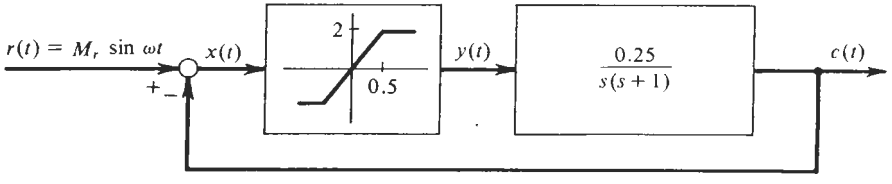

Figure 5-1 *Nonlinear system with saturation.*

5-7. Demonstrate that the TSIDF loci $-1/N_B(A,B,\frac{1}{3},\theta)$ for a cubic nonlinearity are circles described by ($k = B/A$)

$$\text{Center} = \left(-\frac{4}{3A^2} \frac{2 + k^2}{k^4 + 3k^2 + 4}, 0 \right)$$

$$\text{Radius} = \frac{4}{3A^2} \frac{k}{k^4 + 3k^2 + 4}$$

and plot these loci for fixed A at several values of k in the ranges $0 < k < 1$ and $1 < k < 8$.

5-8. By noting that any piecewise-linear limiter with drive levels $\pm D$ and input breakpoints $\pm\delta$ can be represented in terms of a unity drive level, unity breakpoint limiter, preceded by a linear gain $1/\delta$ and followed by a gain D, show that, as a consequence of Fig. 5.2-5, the rule for avoidance of subharmonic oscillations in systems containing a forward-path ideal relay is as illustrated in Fig. 5-2.

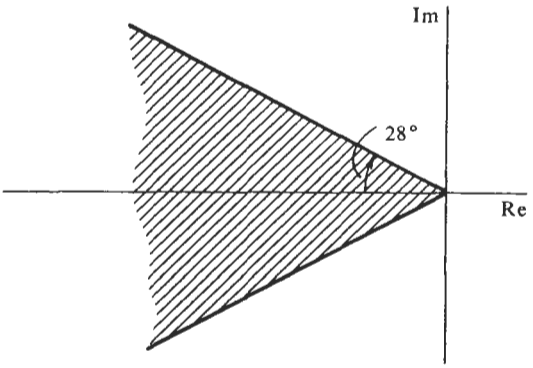

Figure 5-2 The 28° rule for elimination of subharmonics in systems containing an ideal relay.

5-9. The linear elements in an ideal-relay system are characterized by

$$L(s) = \frac{60(0.25s + 1)^2}{s(s + 1)^2(0.05s + 1)^2}$$

Is the high-frequency limit cycle indicated on an amplitude-phase plot of $L(j\omega)$ and $-1/N(A)$ a mode which can exist by itself?

5-10. A certain surface ship has a base-rate–motion-isolated rocket-launching platform. The elements of the platform roll-rate control loop are as illustrated in Fig. 5-3. Under an extremely rough sea condition the roll-rate control-loop disturbing torque signal T_d is given by $T_d = 1.5 \sin t$. Calculate the amplitude of the noise torquing signal at station T due to a 1-volt 400-cps stray pickup signal n.

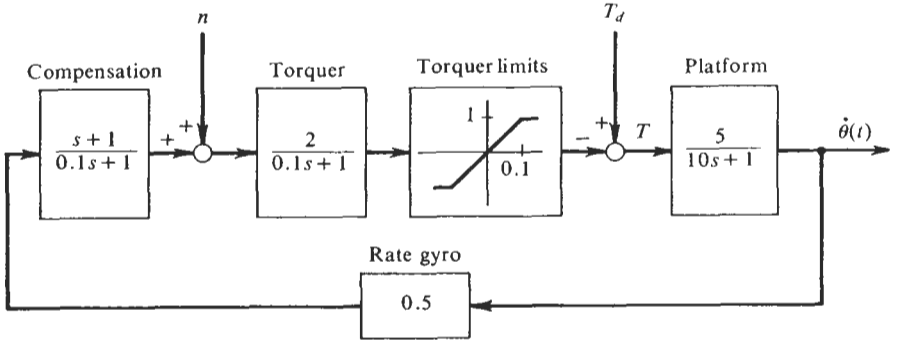

Figure 5-3 Launching platform roll-rate control loop.

5-11. A ground-based missile contains an inertial navigation system with a coarse-leveling loop as illustrated in Fig. 5-4. Instrument errors and gimbal servo dynamics have been neglected; the inertial platform is treated as a pure integrator. The quantity θ is the tilt angle (radians), measured with respect to the local vertical. Because of the effect of wind gusting on the missile structure, the accelerometer senses a disturbance input $d = 0.2g \sin 2\pi t + 0.02g \sin 8\pi t$. The accelerometer has a "notch" of $0.1g$ width and an otherwise linear characteristic of slope 1 volt/g. Calculate θ in terms of two sinusoidal components, and thereby determine the accuracy of this coarse-leveling mode. How can the accuracy be improved?

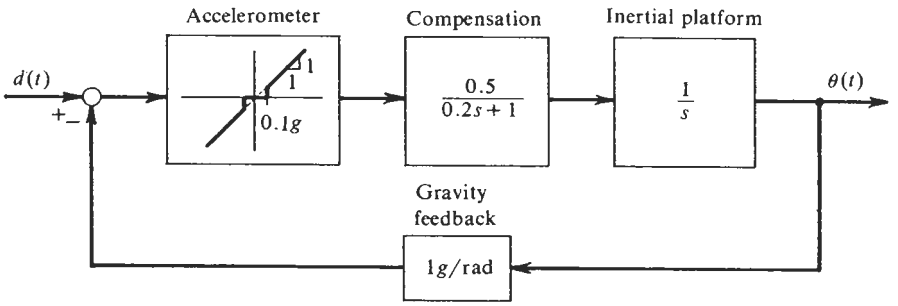

Figure 5-4 *Missile inertial-navigation-system erection loop.*

5-12. For the system of Example 4.4-1, compute the damping factor associated with a limit cycle perturbation by means of the incremental-input describing function. To facilitate an analytic solution to this problem, note that the graphical construction employed can be interpreted as the solution for the intersections between a line and a circle. Compute the slope of the "line" [that is, $L(\sigma + j\omega_0)^{-1}$] at the point where $\sigma = 0$, and thus deduce the approximate result, $\sigma \approx -\zeta\omega_n/(1 + 4\zeta^2)$ for large ζ.

5-13. Derive the incremental-input describing function associated with the kth incremental component of the nonlinearity input

$$x = A \sin \omega t + \sum_{k=1}^{n} \epsilon_k \sin (\omega t + \theta_k)$$

and put it in the standard form

$$N_{ik}(A,\theta_k) = N(A) + \frac{AN'(A)}{2}(1 + e^{-j2\theta_k})$$

5-14. A linear time-varying differential equation of considerable physical importance is the Mathieu equation,

$$\ddot{x} + [\omega_n^2 - M \sin (t + \theta)]x = 0$$

A block diagram appropriate for this system appears in Fig. 5-5. We wish to study the stability of the parametrically excited oscillations of this system by describing function methods.[1]

[1] A. Leonhard, Extension of the Describing Function Method to the Investigation of Parametric Oscillations, *Proc. IFAC*, Basel, Switzerland (August, 1963), pp. 187/1–7.

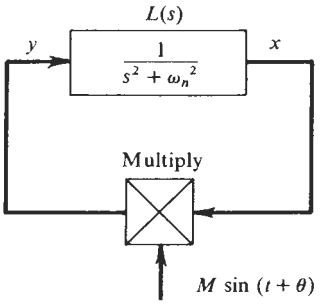

Figure 5-5 *Block diagram of the Mathieu equation.*

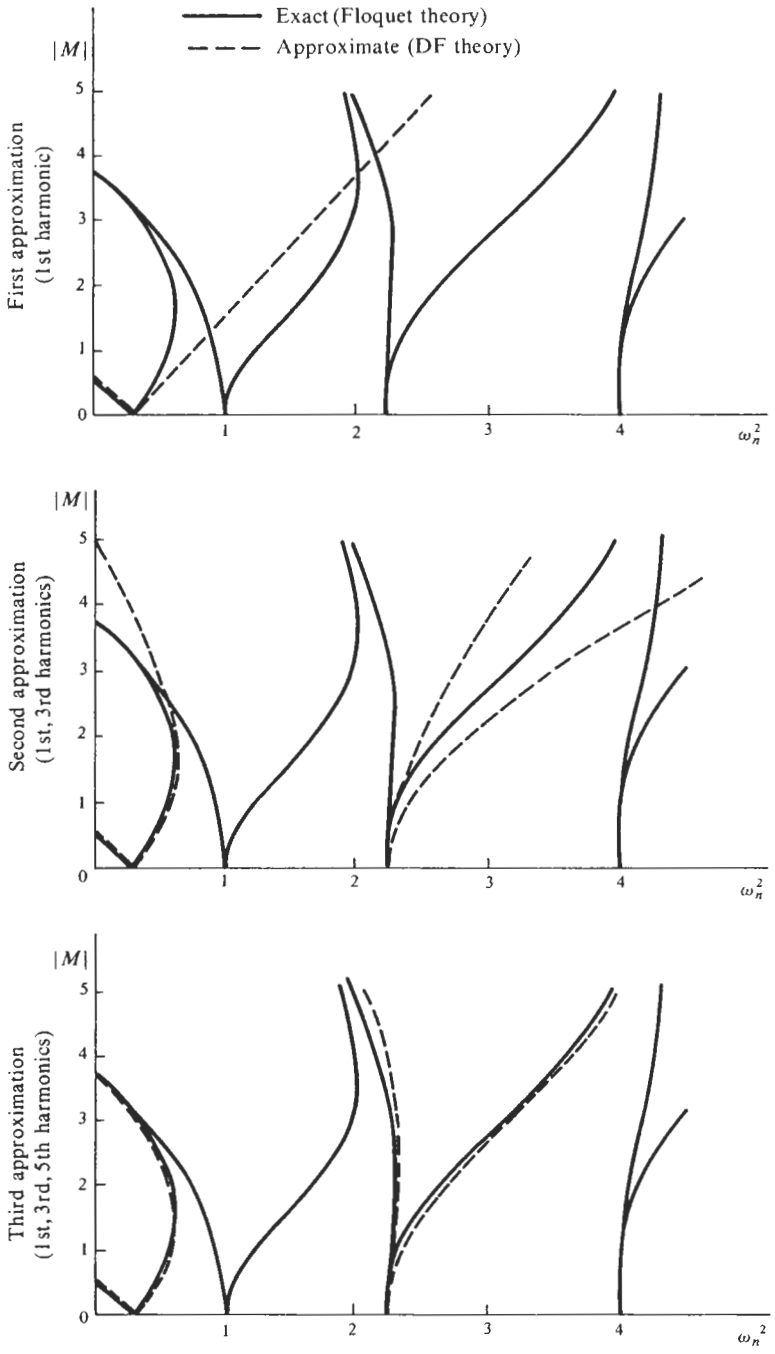

Figure 5-6 *Stability boundaries for the Mathieu equation* ($\omega = \frac{1}{2}$).

(*a*) Assuming the system to be in a state of neutral stability given by

$$x = A \sin \omega t$$

show that an appropriate DF model for the multiplicative gain is

$$N(A,M,\theta) = \frac{M}{2} e^{j(\theta+\pi/2)}$$

(This requires the argument that only $\omega = \frac{1}{2}$ yields solutions of consequence.) Next, invoke the DF requirement for self-sustained system oscillation to find

$$M = 2[\omega_n^2 - (\tfrac{1}{2})^2]$$

This equation for the stability boundary is conventionally plotted in the form $|M|$ versus ω_n^2. Such has been illustrated in Fig. 5-6 against a background of the exact stability boundaries for the Mathieu equation as determined by Floquet theory.

(*b*) Now consider the more representative steady-state self-oscillation waveform

$$x = A_1 \sin \omega t + A_3 \sin (3\omega t + \psi)$$

Show that the appropriate TSIDF model for the multiplicative gain is

$$N_1(A_1,A_3,M,\theta) = \frac{M}{2} e^{j(\theta+\pi/2)} + \frac{MA_3}{2A_1} e^{j(\psi-\theta+\pi/2)}$$

$$N_3(A_1,A_3,M,\theta) = -\frac{MA_1}{2A_3} e^{j(\theta-\psi+\pi/2)}$$

and derive, as the equation for the stability boundary,

$$\left[\frac{M}{2} e^{j(\theta+\pi/2)} + \left(\frac{M}{2}\right)^2 L(j\tfrac{3}{2})\right] L(j\tfrac{1}{2}) = 1$$

with the corresponding solution

$$M = \pm[\omega_n^2 - (\tfrac{3}{2})^2] \pm \sqrt{[\omega_n^2 - (\tfrac{3}{2})^2]^2 + 4[\omega_n^2 - (\tfrac{3}{2})^2][\omega_n^2 - (\tfrac{1}{2})^2]}$$

This result is plotted in Fig. 5-6, where, in addition to an improvement in the shape of the approximately derived solution, *two* distinct V-shaped boundaries appear.

(*c*) Finally, consider the case in which the first, third, and fifth harmonics are included in the self-oscillation waveform model, viz.,

$$x = A_1 \sin \omega t + A_3 \sin (3\omega t + \psi_3) + A_5 \sin (5\omega t + \psi_5)$$

Determine the *three* appropriate describing function gains of the multiplicative term, and demonstrate that the stability-boundary equation takes the form

$$\left[\frac{M}{2} e^{j(\theta+\pi/2)} + \frac{(M/2)^2}{1/[L(j\frac{3}{2})] - (M/2)^2 L(j\frac{5}{2})}\right] L(j\tfrac{1}{2}) = 1$$

The solution of this equation has been plotted in Fig. 5-6, where it is clearly seen that the describing function analysis yields an excellent approximation to the exact solution. A third V-shaped boundary arises from the point $\omega_n^2 = 6.25$, although this is not shown.

5-15. The incorporation of a dc term in the self-oscillation waveform of the parametric oscillator of Prob. 5-14 yields additional stability-boundary solutions of interest.
(*a*) Choose

$$x = A_0 + A_1 \sin \omega t$$

and by following the lead of Prob. 5-14, develop the dc and first-harmonic gains of the multiplicative term (now using the argument that only $\omega = 1$ yields solutions of interest), and by manipulating, obtain the results

$$M \text{ is arbitrary} \qquad \text{for } \omega_n^2 = 1$$

$$M = \sqrt{2\omega_n^2(\omega_n^2 - 1)} \qquad \text{for } \omega_n^2 > 1$$

(*b*) Show that for the three-term waveform model

$$x = A_0 + A_1 \sin \omega t + A_2 \sin (2\omega t + \psi_2)$$

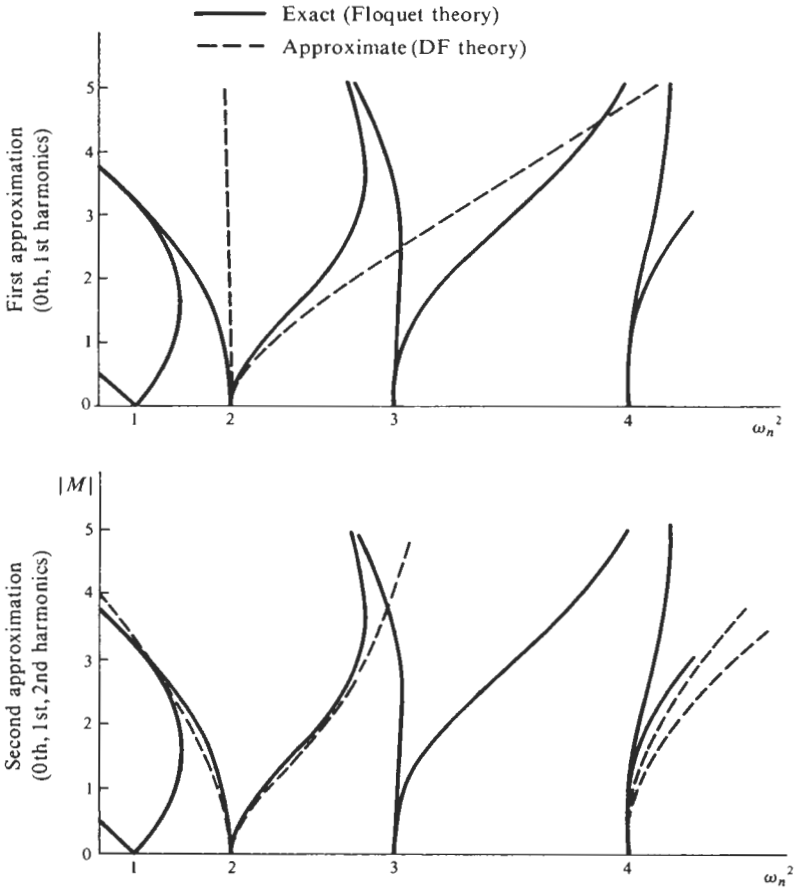

Figure 5-7 *Stability boundaries for the Mathieu equation* ($\omega = 1$).

the stability-boundary solutions are

$$M = \begin{cases} 2\sqrt{\omega_n^2 - 1}\sqrt{\omega_n^2 - 4} & \text{for } 1 > \omega_n^2 > 4 \\ 2\sqrt{\dfrac{\omega_n^2(\omega_n^2 - 1)(\omega_n^2 - 4)}{3\omega_n^2 - 8}} & \text{for } 1 < \omega_n^2 < \tfrac{8}{3} \quad \text{and} \quad \omega_n^2 > 4 \end{cases}$$

These approximate solutions are plotted in Fig. 5-7. Note that the boundaries arising under the assumption $\omega = 1$ with a self-oscillation waveform dc term are located in between the boundaries determined under the assumption $\omega = \frac{1}{2}$ without a dc term.

5-16. Make an argument which demonstrates that the area between the stability boundaries and the abscissa corresponds to the region of *stable* operation, whereas that above the boundaries denotes *unstable* operation, for the Mathieu equation.

5-17. For the system of Fig. 5-8, find the region in the space of M_r and ω in which the system would display a stable response to the sinusoidal input, and would not limit-cycle.

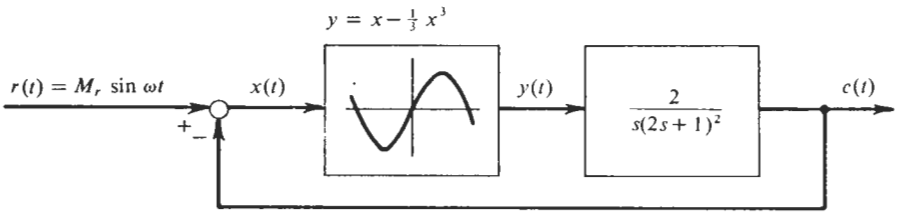

Figure 5-8

5-18. Write a general expression for the steady-state response $c(t)$ to the sinusoidal input for the system of Fig. 5-9—an expression valid for all combinations of input amplitude and frequency resulting in a response at x which is of small amplitude relative to the amplitude of the limit cycle at x.

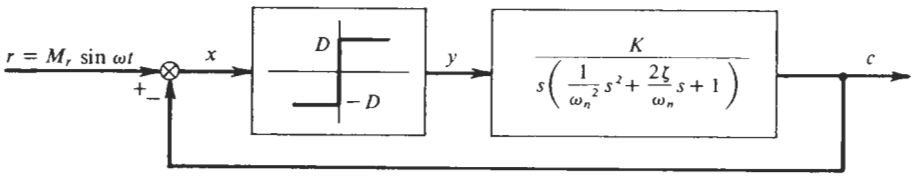

Figure 5-9

5-19. For a cubic nonlinearity, $y = x^3$, show that the *three*-sinusoid-input describing function gains corresponding to the input

$$x(t) = A_1 \sin \omega t + A_3 \sin (3\omega t + \theta_3) + A_5 \sin (5\omega t + \theta_5)$$

are:[1]

$$N_{A_1} = \frac{3}{4}\left\{\left[A_1^2 + 2A_3^2 + 2A_5^2 - A_1A_3\cos\theta_3 - \frac{A_3^2A_5}{A_1}\cos(2\theta_3 - \theta_5) - 2A_3A_5\cos(\theta_5 - \theta_3)\right] + j\left[-A_1A_3\sin\theta_3 + \frac{A_3^2A_5}{A_1}\sin(2\theta_3 - \theta_5) - 2A_3A_5\sin(\theta_5 - \theta_3)\right]\right\}$$

$$N_{A_3} = \frac{3}{4}\left\{\left[2A_1^2 + A_3^2 + 2A_5^2 - \frac{A_1^3}{3A_3}\cos\theta_3 - \frac{A_1^2A_5}{A_3}\cos(\theta_5 - \theta_3) + 2A_1A_5\cos(\theta_5 - 2\theta_3)\right] + j\left[\frac{A_1^3}{3A_3}\sin\theta_3 - \frac{A_1^2A_5}{A_3}\sin(\theta_5 - \theta_3) + 2A_1A_5\sin(\theta_5 - 2\theta_3)\right]\right\}$$

$$N_{A_5} = \frac{3}{4}\left\{\left[2A_1^2 + 2A_3^2 + A_5^2 - \frac{A_1^2A_3}{A_5}\cos(\theta_5 - \theta_3) + \frac{A_1A_3^2}{A_5}\cos(2\theta_5 - \theta_3)\right] + j\left[-\frac{A_1^2A_3}{A_5}\sin(\theta_3 - \theta_5) + \frac{A_1A_3^2}{A_5}\sin(2\theta_3 - \theta_5)\right]\right\}$$

5-20. A nonlinear feedback system is comprised of a cubic nonlinearity, $y = x^3$, and fourth-order linear elements

$$L(s) = \frac{10s^2}{[(s + 0.01)^2 + 0.9^2][(s + 0.01)^2 + 1.1^2]}$$

(*a*) Show that DF arguments lead to the conclusion that the system does not limit-cycle. Based upon consideration of the shape of the $L(j\omega)$ locus, would you *suspect* the DF conclusion to be in error?

(*b*) Now assume a nonlinearity input of the form

$$x(t) = A_1\sin\omega t + A_3\sin(3\omega t + \theta)$$

and by simultaneously satisfying the four conditions

$$|N_{A_1}|\,|L(j\omega)| = 1 \qquad \angle N_{A_1} + \angle L(j\omega) = \pm\pi$$
$$|N_{A_3}|\,|L(j3\omega)| = 1 \qquad \angle N_{A_3} + \angle L(j3\omega) = \pm\pi$$

show that this TSIDF argument *does* predict a limit cycle, given by

$$x(t) = 1.13\sin 0.608t + 0.605\sin(1.824t + 0.083)$$

This oscillator problem is one of a class of problems studied by Fitts, who showed that *several* modes of oscillation can indeed occur. The *first mode*, in which the predominant harmonic is the third, was measured as

$$x(t) = 1.13\sin 0.604t + 0.548\sin(1.812t + 0.093)$$

(*c*) Outline how you would solve for the so-called *second mode* of oscillation, in which the first, third, and fifth harmonics appear?

[1] Fitts, R. E.: Linearization of Nonlinear Feedback Systems, Ph.D. thesis, Massachusetts Institute of Technology, Cambridge, Mass., June, 1966.